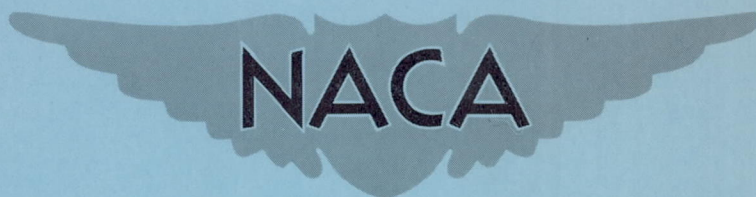


CASE FILE RM L51C07  
COPY

NACA RM L51C07



# RESEARCH MEMORANDUM

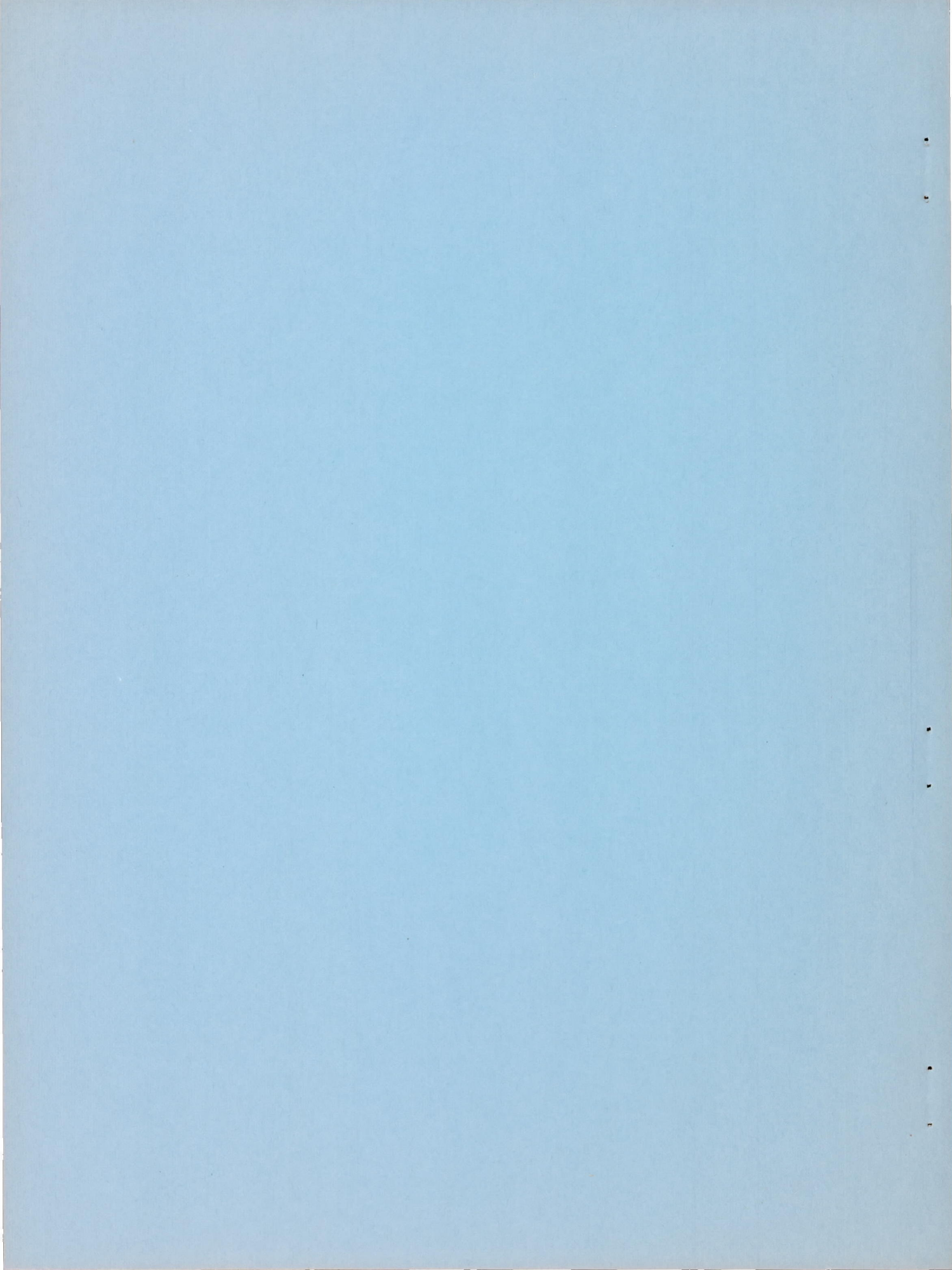
EFFECT OF A DEFLECTABLE WING-TIP CONTROL ON THE LOW-SPEED  
LATERAL AND LONGITUDINAL CHARACTERISTICS OF A  
LARGE-SCALE WING WITH THE LEADING  
EDGE SWEPT BACK  $47.5^\circ$

By Roy H. Lange and Marvin P. Fink

Langley Aeronautical Laboratory  
Langley Field, Va.

NATIONAL ADVISORY COMMITTEE  
FOR AERONAUTICS  
WASHINGTON

April 26, 1951  
Declassified August 31, 1954





## NATIONAL ADVISORY COMMITTEE FOR AERONAUTICS

## RESEARCH MEMORANDUM

EFFECT OF A DEFLECTABLE WING-TIP CONTROL ON THE LOW-SPEED

LATERAL AND LONGITUDINAL CHARACTERISTICS OF A

LARGE-SCALE WING WITH THE LEADING

EDGE SWEEPED BACK  $47.5^\circ$ 

By Roy H. Lange and Marvin P. Fink

## SUMMARY

Results are presented of an investigation in the Langley full-scale tunnel of the effect of a 20-percent-semispan deflectable wing-tip control on the low-speed lateral and longitudinal characteristics of a wing with the leading edge swept back  $47.5^\circ$ , an aspect ratio of 3.5, and circular-arc-airfoil sections. Limited tests were also made of a conventional aileron simulated by an outboard 50-percent-semispan, 20-percent-chord trailing-edge plain flap (for positive deflections only). The basic wing configuration, the wing with drooped-nose flaps deflected  $40^\circ$ , and the wing with drooped-nose and semispan plain flaps deflected  $40^\circ$  were tested in the course of the investigation. All the data are presented for a Reynolds number of  $4.3 \times 10^6$  and a Mach number of 0.07.

The results show that the 20-percent-semispan wing-tip control investigated should provide adequate lateral control over the angle-of-attack range investigated. For the basic wing the wing-tip control was about as effective as a 50-percent-semispan trailing-edge aileron throughout the angle-of-attack range. With flaps deflected, the effectiveness of the wing-tip control was greater than that of the trailing-edge aileron at the higher angles of attack. Equal (trailing edge up) deflection of the wing-tip controls provided an improvement in the flow over the wing throughout the angle-of-attack range for all configurations. Deflection of the wing-tip controls resulted in a nose-up trim change for all wing configurations. The lift-to-drag ratio of the wing at 0.85 maximum lift with tips neutral is 3.8 for the basic wing, 5.2 for the wing with drooped-nose flaps deflected, and 6.1 for the wing with drooped-nose and semispan plain flaps deflected. With the wing-tip controls deflected  $-15^\circ$ , these values become 3.7, 7.5, and 7.0, respectively.

## INTRODUCTION

Wing-tip ailerons have shown favorable rolling effectiveness characteristics as compared with trailing-edge ailerons on sweptback- and delta-wing configurations throughout the transonic and low supersonic speed range (references 1 and 2). There are little data existent, however, relative to the effectiveness of wing-tip ailerons on sweptback wings at low speeds. Some previous investigations at low speeds and small scale (reported in reference 3) have been confined to a wing of very low aspect ratio. The wing-tip control of the subject wing appeared promising because of the longer rolling-moment arm inherent with all tip-aileron devices and because of the possibility of alleviating tip stalling throughout the angle-of-attack range by negative (trailing edge up) deflections of both tips.

An investigation has been made in the Langley full-scale tunnel of the lateral and longitudinal characteristics of a large-scale wing of aspect ratio 3.5 with the leading edge swept back  $47.5^\circ$  and with the outer 20 percent of each wing semispan deflectable about a hinge axis normal to the plane of symmetry. The wing-tip control used in the present investigation differs, therefore, from that used in previous investigations (references 1 and 3) in that a portion of the wing is deflected, whereas the tip controls used previously consist of small surfaces attached to the tips of the existing wings.

Force data are presented herein at a Reynolds number of  $4.3 \times 10^6$  and a Mach number of 0.07, from tests made to determine the effectiveness of the 20-percent-semispan wing-tip controls for angles of attack through stall and for total (differential) wing-tip-control deflections ranging from  $0^\circ$  to  $50^\circ$ . For a limited comparison, tests were made of a conventional aileron simulated by an outboard 50-percent-semispan, 20-percent-chord trailing-edge plain flap for positive deflections only. Data are also presented of the longitudinal aerodynamic characteristics of the wing with both wing-tip controls deflected in the same direction for several negative (trailing edge up) deflections at each angle of attack. The basic wing configuration, the wing with the drooped-nose flaps deflected  $40^\circ$ , and the wing with the drooped-nose and inboard semispan plain flaps deflected  $40^\circ$  were tested in the course of the investigation. In addition to the force measurements, the stalling characteristics of the wing with the wing-tip controls deflected in the same direction were determined by means of tuft observations.



## COEFFICIENTS AND SYMBOLS

The test data are presented as standard NACA coefficients of forces and moments. The data are referred to a set of axes coinciding with the wind axes, and the origin was located in the plane of symmetry as projected from the quarter-chord point of the mean aerodynamic chord.

$C_L$	lift coefficient ( $L/qS$ )
$C_D$	drag coefficient ( $D/qS$ )
$C_m$	pitching-moment coefficient ( $M/qS\bar{c}$ )
$C_{l_T}$	rolling-moment coefficient with wing-tip control deflected (Rolling moment/ $qSb$ )
$C_{n_T}$	yawing-moment coefficient with wing-tip control deflected ( $N/qSb$ )
$C_{l_a}$	rolling-moment coefficient produced by the trailing-edge aileron
$C_{n_a}$	yawing-moment coefficient produced by the trailing-edge aileron
$L/D$	lift-drag ratio
$C_{L_{max}}$	maximum lift coefficient
$pb/2V$	wing-tip helix angle, radians
$C_{l_p}$	damping-in-roll coefficient; rate of change of rolling-moment coefficient with wing-tip helix angle $\left(\frac{\partial C_l}{\partial \frac{pb}{2V}}\right)$
$R$	Reynolds number
$L$	lift
$D$	drag
$M$	pitching moment
$N$	yawing moment

$x_{ac}$	approximate aerodynamic-center location, percent $\bar{c}$ $\left(0.25 - \frac{dC_m}{dC_L}\right)100$
$\alpha$	angle of attack measured in plane of symmetry, degrees
$q$	free-stream dynamic pressure
$S$	wing area (231.0 sq ft)
$p$	angular velocity about X-axis
$b$	wing span (28.5 ft)
$\bar{c}$	mean aerodynamic chord measured parallel to plane of symmetry (8.37 ft) $\left(\frac{2}{S} \int_0^{b/2} c^2 dy\right)$
$V$	free-stream velocity
$\delta_{Tt}$	wing-tip-control deflection, positive with trailing edge down, degrees
$\delta_{T_t}$	total (equal up and down) wing-tip-control deflection, degrees
$\delta_{aR}$	right trailing-edge-aileron deflection, positive for down deflections, degrees
$c$	chord, parallel to plane of symmetry
$c'$	chord, perpendicular to line of maximum thickness
$y$	spanwise coordinate perpendicular to plane of symmetry
$C_{L\alpha}$	rate of change of lift coefficient with angle of attack $(\partial C_L / \partial \alpha)$ , per degree
$dC_m / dC_L$	rate of change of pitching-moment coefficient with lift coefficient
$C_l \delta_{T_t}$	rate of change of rolling-moment coefficient with wing-tip- control deflection $(\partial C_l / \partial \delta_{T_t})$ , per degree



## MODEL

The geometric characteristics of the wing with respect to the unswept wing panel are given in figure 1. The wing has an angle of sweepback of  $45^\circ$  at the quarter-chord line, an aspect ratio of 3.5, a taper ratio of 0.5, and has no geometric dihedral or twist. The airfoil section of the wing is a symmetrical, 10-percent-thick, circular-arc section perpendicular to the 50-percent-chord line. The wing was constructed of  $\frac{1}{4}$ -inch aluminum sheet reinforced by steel channel spars. The wing construction is extremely rigid and it is believed that no deflections of an appreciable magnitude occurred during the tests.

The wing is equipped with a full-span drooped-nose flap and an inboard semispan plain flap which are 20 percent of the chord measured perpendicular to the line of maximum thickness. These flaps are pivoted on piano hinges mounted flush with the lower wing surface and, when deflected, produce a gap on the upper wing surface which is covered and faired with a sheet metal seal.

The wing-tip-control configuration tested consists of the outer 20 percent of each wing semispan deflectable about a hinge axis normal to the plane of symmetry and at 0.54c. (See figs. 1 and 2.) Deflections of from  $30^\circ$  to  $-40^\circ$  are possible, and the deflections are remotely controlled by actuators within the wing. The tips can be deflected differentially as ailerons or in the same direction as flaps. The gap at the juncture between the wing-tip control and the wing is about  $\frac{3}{16}$  inch throughout. The area of each wing-tip control is equivalent to 14.4 percent of the area of the wing semispan.

The trailing-edge aileron tested is an outboard 50-percent-semispan, 20-percent-chord (normal to the 50-percent-chord line) trailing-edge plain flap. Downward deflections of  $0^\circ$ ,  $5.7^\circ$ ,  $10.2^\circ$ ,  $14.3^\circ$ , and  $19.6^\circ$  are provided on the right aileron only, and when the aileron is deflected the gap on the upper wing surface is sealed and faired. The area of the right trailing-edge aileron is equivalent to 10.9 percent of the area of the wing semispan.

## TESTS

The tests were made through a maximum angle-of-attack range from about  $0^\circ$  to  $29^\circ$  and at a Reynolds number of  $4.3 \times 10^6$  and a Mach number of 0.07. Three wing configurations were tested: the basic wing configuration, the wing with the drooped-nose flaps deflected  $40^\circ$ , and

the wing with both the drooped-nose and inboard semispan plain flaps deflected  $40^\circ$ . The drooped-nose flap configuration was investigated because the results of the pressure-distribution measurements over the wing (reference 4) showed that the vortex-type flow, inherent for the basic wing configuration, was eliminated by  $40^\circ$  deflection of the full-span drooped-nose flap. With the tip control deflected the span of the drooped-nose flap extended from the plane of symmetry outboard to 80 percent of the wing semispan.

For the tests made to determine the effectiveness of the wing-tip controls deflected as ailerons, the tips were first deflected in equal amounts in a leading-edge down direction at each angle of attack until the spanwise flow at the tips disappeared; then the tips were deflected differentially in  $5^\circ$  increments. The deflections used at each angle of attack about which the wing-tip controls were deflected differentially are given in table I for each wing configuration. The maximum negative deflection for these tests was limited to  $-20^\circ$ . The aileron-effectiveness tests of the trailing-edge aileron were made with only the right aileron deflected through a range from  $0^\circ$  to  $19.6^\circ$ . For these tests the aileron was set at the required deflection, and then force tests were made as the angle of attack of the wing was increased through a maximum range of from  $0^\circ$  to  $29^\circ$ .

In order to determine the effect of wing-tip-control deflection on the longitudinal aerodynamic characteristics of the wing, the tips were deflected negatively in the same direction in  $5^\circ$  increments at each angle of attack until no further improvement in the flow over the tips was observed. The effects of negative tip deflection on the stall progression of the wing were determined from visual observations of the action of wool tufts attached to the upper wing surface.

Throughout the investigation there was no evidence of vibration or flutter of the wing-tip control regardless of the wing attitude or tip deflection tested.

## RESULTS AND DISCUSSION

### Presentation of Results

The results have been corrected for the blocking effects, tares, and for approximate wing-support interference. The angles of attack and drag coefficients have been corrected for jet-boundary effects by the method given in reference 5. In addition, the angles of attack have been corrected for air-stream misalignment.



The results of the investigation are presented in two sections. The first section presents the aerodynamic characteristics of the wing with the wing-tip controls deflected as ailerons. The basic data are given in figures 3 to 5. The rolling and yawing moments for a total aileron deflection of  $40^\circ$  are presented in figure 6, and the rolling effectiveness for the basic wing is given in figure 7. The characteristics of the 0.50b/2 trailing-edge aileron are presented in figures 8 and 9 for comparison purposes. The effectiveness parameters ( $C_{l\delta}$ ) for the two aileron configurations are given in table II. The second section presents the effects of the wing-tip control on the longitudinal characteristics of the wing with the tips deflected in the same direction. The basic data are given in figures 10 to 16. Diagrams showing the effect of wing-tip-control deflection on the stalling characteristics are given in figures 11, 12, and 13. The summary curves (figs. 17 and 18) show the effect of wing-tip-control deflection on the approximate aerodynamic-center location and on the lift-drag ratio.

#### Effect of Tip Control on Lateral Characteristics

Tip-control effectiveness.- The wing-tip controls at each angle of attack were differentially deflected about an initial deflection which was not coincident with the chord line of the wing. (See table I.) The wing-tip-control effectiveness parameter  $C_{l\delta_{Tt}}$  for the basic wing increases from -0.00085 at the lowest angle of attack to -0.00100 at  $\alpha = 14.2^\circ$  and then decreases to -0.00070 near maximum lift. (See fig. 3 and table II.) The effectiveness parameter at the lowest angle of attack compares favorably with the value of -0.00088 calculated by the method of reference 6 for a trailing-edge plain aileron of 50-percent semispan and 20-percent chord.

The 0.80b/2 drooped-nose flaps increased the wing-tip-control effectiveness in the high angle-of-attack range as compared with the basic wing. (See fig. 4 and table II.) The highest values of the wing-tip-control effectiveness parameter (-0.00113) were measured in the high angle-of-attack range for the wing with the 0.80b/2 drooped-nose flaps and semispan plain flaps deflected (fig. 5 and table II).

Rolling- and yawing-moment characteristics.- As an indication of the effectiveness of the wing-tip control in the high deflection range, the rolling-moment coefficients produced by a total wing-tip-control deflection of  $40^\circ$  are plotted against angle of attack in figure 6 for the three wing configurations. In the low angle-of-attack range the rolling-moment coefficient was about 0.04 for all configurations. The effect of the 0.80b/2 drooped-nose flaps was to prevent the large loss in rolling-moment coefficient near maximum lift that was noted for the

basic wing and to provide an increase in the rolling-moment coefficients in the moderate angle-of-attack range. For the wing with the combined deflections of the drooped nose and plain flaps, there is a rapid decrease in rolling-moment coefficient with increase in angle of attack above  $14^\circ$ .

As shown in figure 6, the favorable yawing-moment coefficients of the basic wing caused by wing-tip-control deflection at the low angles of attack are increased and extended to moderate angles of attack by the addition of the flaps. In the high angle-of-attack range the adverse yaw is increased by the flaps.

Rolling effectiveness.- In order to indicate a measure of the rolling effectiveness of the wing-tip control investigated, values of the wing-tip helix angle  $pb/2V$  have been calculated for the basic wing configuration. The estimated values of  $pb/2V$  were determined from the relationship  $\frac{pb}{2V} = \frac{C_l}{C_{l_p}}$ . The values of  $C_{l_p}$  were determined from the expression

$$C_{l_p} = (C_{l_p})_{C_L=0} \frac{(C_{L_\alpha})_{C_L}}{(C_{L_\alpha})_{C_L=0}}$$

given as method 1 in reference 7. The value of  $(C_{l_p})_{C_L=0}$  for the wing as determined from the charts of reference 6 was  $-0.265$ . The values of  $pb/2V$  presented have not been corrected for the effects of adverse yaw or wing twist, and an aileron linkage system giving a differential of 1:1 (equal up and down deflections) is assumed.

The data of figure 7 show that the total wing-tip-control deflection required to produce a helix angle of  $0.09$ , considered necessary for satisfactory low-speed control as specified in reference 8, increases from  $27^\circ$  at  $\alpha = 3.0^\circ$  to  $32.5^\circ$  at  $\alpha = 6.7^\circ$  and then decreases to  $20^\circ$  at  $\alpha = 14.2^\circ$ . The large increase in the values of  $pb/2V$  at an angle of attack of  $14.2^\circ$  is similar to that shown in reference 9 for the effect of an end plate on the effectiveness of a tip-aileron control.

Lift and pitching-moment characteristics.- The data of figures 3, 4, and 5 show that increasing the total wing-tip-control deflection



from  $0^\circ$  to  $40^\circ$  has a slight effect on the lift and pitching-moment characteristics. However, as shown in figures 3(b), 4(b), and 5(b), there is a lift and trim change associated with the initial wing-tip-control deflection at each angle of attack. It is estimated that the maximum change in trim associated with the initial wing-tip-control deflection for each configuration would amount to about  $12^\circ$  of elevator deflection for an unswept tail and a dynamic pressure ratio of 1.00.

Comparison with trailing-edge plain aileron.- The rolling- and yawing-moment coefficients for the  $0.50b/2$  trailing-edge plain aileron presented in figures 8 and 9 represent the coefficient at a given deflection minus the coefficient at zero deflection. The data from which the rolling-moment coefficients for the basic wing were derived are given in reference 10 and are typical of the data obtained for the other wing configurations. In the following discussion it should be noted that the hinge line of the trailing-edge aileron is swept back  $36^\circ$ , whereas the hinge line of the wing-tip control is unswept, and also that the trailing-edge aileron has less area than the wing-tip control.

A comparison of the data of figures 3, 4, 5, and 8 shows that the variation of rolling-moment coefficient with wing-tip-control deflection is almost linear with the tip controls deflected, whereas the variation with the trailing-edge aileron deflected is irregular and in many cases shows a reversed effectiveness. This irregular variation of rolling-moment coefficient with trailing-edge-aileron deflection was investigated in reference 10, and it was found that a more nearly linear variation was produced by application of finite-trailing-edge thickness to the ailerons.

The aileron effectiveness parameters for the two aileron configurations (table II) are about the same at the low and high angles of attack for the basic wing configurations. For the configurations with flaps deflected, however, the effectiveness of the wing-tip control increases over that measured for the trailing-edge aileron with increasing angle of attack. For the configuration with the drooped-nose and plain flaps deflected, the tip-control effectiveness is about twice that measured for the trailing-edge aileron. It should be noted, however, that the trailing-edge aileron was deflected downward only and that upward deflections might cause a slight change in the average slope of the curves through zero deflection.

An indication of the effect of airfoil section on the aileron characteristics of the wing plan form under consideration may be obtained from the data of reference 11 for a wing-fuselage combination of almost identical plan form and sweepback but with an NACA 64<sub>1</sub>A112 airfoil section. The aileron effectiveness parameter of the basic wing

configuration near maximum lift for the wing-tip control and  $0.50b/2$  trailing-edge aileron on the subject wing is  $-0.00070$ , whereas the value for a  $0.45b/2$  aileron of reference 11 near maximum lift is  $-0.00050$ . It should also be noted that for the wing with flaps deflected, the effectiveness of the wing-tip control is considerably higher than that measured for the  $0.45b/2$  aileron of reference 11 in the high angle-of-attack range.

### Effect of Wing-Tip-Control Deflection on

#### Longitudinal Characteristics

It was believed that by equal deflection of both wing-tip controls the vortex flow, inherent for the basic wing (reference 4), could be modified somewhat in the region of the tips and that some improvement in the lift and pitching-moment characteristics would be realized. Comparisons of the flow over the wing, both with the wing-tip controls neutral and with the wing-tip controls deflected in the same direction, are given in figures 11 to 13. As shown in figures 11 to 13, negative wing-tip-control deflection provided an improvement in the flow over the wing throughout the angle-of-attack range for all configurations. Wing-tip-control deflection caused a reduction in lift coefficient throughout the angle-of-attack range for the basic wing configuration. (See fig. 14(a).) In the high angle-of-attack range for the wing with the flaps deflected, the wing-tip-control deflection can be increased to  $-15^\circ$  before any decrease in lift is noted. (See figs. 15(a) and 16(a).)

Negative tip-control deflection caused a change in trim in a positive direction for all configurations. (See figs. 14(a), 15(a), and 16(a).) For the wing with flaps deflected the change in trim caused by wing-tip-control deflection is in a direction which reduces the out-of-trim moment produced by flap deflection. The basic wing has an undesirable shift in aerodynamic center of 25 percent of the mean aerodynamic chord throughout the lift-coefficient range to  $0.85C_{L_{max}}$ . (See fig. 17.) Deflecting the wing-tip controls  $-5^\circ$  reduced this shift in aerodynamic center to about 14 percent for the same lift-coefficient range. No improvement is noted for higher wing-tip-control deflections. For the wing with flaps deflected, the rapid unstable shift in aerodynamic center is delayed to higher lift coefficients with the wing-tip controls deflected  $-15^\circ$ . (See figs. 17, 15(a), and 16(a).)

The lift-drag ratio of the basic wing is decreased with increasing wing-tip-control deflection. At 85-percent maximum lift, however, the lift-drag ratio is decreased from 3.8 to only 3.7 for a wing-tip-control



deflection of  $-15^{\circ}$ . At 85-percent maximum lift the 0.80b/2 drooped-nose flaps increase the lift-drag ratio of the wing to 5.2 with tips neutral. Wing-tip-control deflection provides a further increase in lift-drag ratio in the moderate- to high-lift-coefficient range, and at 85-percent maximum lift a value of 7.5 is measured for a wing-tip-control deflection of  $-15^{\circ}$ . (See fig. 18(b).) Deflecting the rear flaps in combination with the drooped-nose flaps increases the lift-to-drag ratio to 6.1 for the tips-neutral condition. At 85-percent maximum lift, wing-tip-control deflection of  $-15^{\circ}$  further increases the lift-drag ratio to 7.0. (See fig. 18(c).)

#### SUMMARY OF RESULTS

The results of an investigation in the Langley full-scale tunnel of the effect of a 20-percent-semispan deflectable wing-tip control on the low-speed lateral and longitudinal characteristics of a wing with the leading edge swept back  $47.5^{\circ}$  and circular-arc-airfoil sections showed the following:

1. The 20-percent-semispan wing-tip control investigated should provide adequate lateral control over the angle-of-attack range investigated for the basic wing as well as for the wing with flaps deflected.
2. For the basic wing the aileron effectiveness parameter for the wing-tip control was about the same as that for the 50-percent-semispan trailing-edge aileron throughout the angle-of-attack range. With flaps deflected, the effectiveness parameter for the wing-tip control increased over that measured for the trailing-edge aileron with increasing angle of attack. The highest values of aileron effectiveness parameter for the wing-tip control were measured at the high angles of attack with flaps deflected.
3. Equal negative deflection of the wing-tip controls provided an improvement in the flow over the wing throughout the angle-of-attack range for all configurations.
4. As compared to the wing with tips neutral, wing-tip-control deflection in the high angle-of-attack range caused a decrease in lift for the basic wing, but for the wing with flaps deflected, the wing-tip-control deflection can be increased to  $-15^{\circ}$  before a decrease in lift is produced.
5. Negative wing-tip-control deflection caused a change in trim in a positive direction for all configurations.

6. The lift-drag ratio of the wing at 85-percent maximum lift with tips neutral is 3.8 for the basic wing, 5.2 for the wing with drooped-nose flaps deflected, and 6.1 for the wing with drooped-nose and semi-span plain flaps deflected. With the wing-tip controls deflected  $-15^{\circ}$ , these values become 3.7, 7.5, and 7.0, respectively.

Langley Aeronautical Laboratory  
National Advisory Committee for Aeronautics  
Langley Field, Va.



## REFERENCES

1. Sandahl, Carl A., Strass, H. Kurt, and Piland, Robert O.: The Rolling Effectiveness of Wing-Tip Ailerons As Determined by Rocket-Powered Test Vehicles and Linear Supersonic Theory. NACA RM L50F21, 1950.
2. Sandahl, Carl A., and Strass, H. Kurt: Comparative Tests of the Rolling Effectiveness of Constant-Chord, Full-Delta, and Half-Delta Ailerons on Delta Wings at Transonic and Supersonic Speeds. NACA RM L9J26, 1949.
3. Hagerman, John R., and O'Hare, William M.: Investigation of Extensible Wing-Tip Ailerons on an Untapered Semispan Wing at  $0^\circ$  and  $45^\circ$  Sweepback. NACA RM L9H04, 1949.
4. Lange, Roy H., Whittle, Edward F., Jr., and Fink, Marvin P.: Investigation at Large Scale of the Pressure Distribution and Flow Phenomena over a Wing with the Leading Edge Swept Back  $47.5^\circ$  Having Circular-Arc Airfoil Sections and Equipped with Drooped-Nose and Plain Flaps. NACA RM L9G15, 1949.
5. Katzoff, S., and Hannah, Margery E.: Calculation of Tunnel-Induced Upwash Velocities for Swept and Yawed Wings. NACA TN 1748, 1948.
6. Lowry, John G., and Schneiter, Leslie E.: Estimation of Effectiveness of Flap-Type Controls on Sweptback Wings. NACA TN 1674, 1948.
7. Goodman, Alex, and Adair, Glenn H.: Estimation of the Damping in Roll of Wings through the Normal Flight Range of Lift Coefficient. NACA TN 1924, 1949.
8. Anon: Flying Qualities of Piloted Airplanes. U. S. Air Force Specification No. 1815-B, June 1, 1948.
9. Fischel, Jack, and Watson, James M.: Low-Speed Investigation of Deflectable Wing-Tip Ailerons on an Untapered  $45^\circ$  Sweptback Semi-span Wing with and without an End Plate. NACA RM L9J28, 1949.
10. Lange, Roy H.: Full-Scale Investigation of a Wing with the Leading Edge Swept Back  $47.5^\circ$  and Having Circular-Arc and Finite-Trailing-Edge-Thickness Ailerons. NACA RM L9B02, 1949.
11. Pasamanick, Jerome, and Sellers, Thomas B.: Low-Speed Investigation of the Effect of Several Flap and Spoiler Ailerons on the Lateral Characteristics of a  $47.5^\circ$  Sweptback-Wing - Fuselage Combination at a Reynolds Number of  $4.4 \times 10^6$ . NACA RM L50J20, 1950.

TABLE I.- INITIAL DEFLECTIONS FOR WING-TIP-CONTROL  
EFFECTIVENESS TESTS

Configuration	$\alpha$ (deg)	$\delta_T$ (deg)
Basic wing	3.0	-5
	6.7	-10
	10.4	-10
	14.2	-15
	18.0	-20
	22.0	-20
	24.0	-20
0.80b/2 drooped-nose flaps deflected 40°	6.9	-10
	10.6	-15
	14.3	-20
	18.1	-20
	21.9	-20
	25.6	-20
0.80b/2 drooped-nose and 0.50b/2 plain flaps deflected 40°	4.5	-10
	8.2	-15
	13.9	-20
	16.8	-20
	21.5	-20





TABLE II.- COMPARISON OF AILERON EFFECTIVENESS PARAMETERS ( $C_{l\delta}$ )  
 FOR WING-TIP CONTROLS AND TRAILING-EDGE AILERONS  
 [Slopes measured at 0° aileron deflection]

$\alpha$ (deg)	Tip control	Trailing-edge aileron
(a) Basic wing configuration		
3.0	-0.00085	-0.00087
6.7	-.00077	-.00084
10.4	-.00092	-.00084
14.2	-.00100	-.00077
18.1	-.00065	-.00072
22.0	-.00070	-.00070
(b) Drooped-nose flap deflected 40°		
6.9	-0.00079	-0.00070
10.6	-.00066	-.00069
14.4	-.00091	-.00060
18.1	-.00087	-.00065
21.8	-.00097	-.00075
25.7	-.00080	-.00055
27.6	-.00105	
(c) Drooped-nose and semispan plain flaps deflected 40°		
4.5	-0.00070	-0.00043
8.3	-.00094	-.00042
13.9	-.00084	-.00045
16.7	-.00113	-.00042
19.6	-.00083	-.00032
21.6	-.00113	-.00060

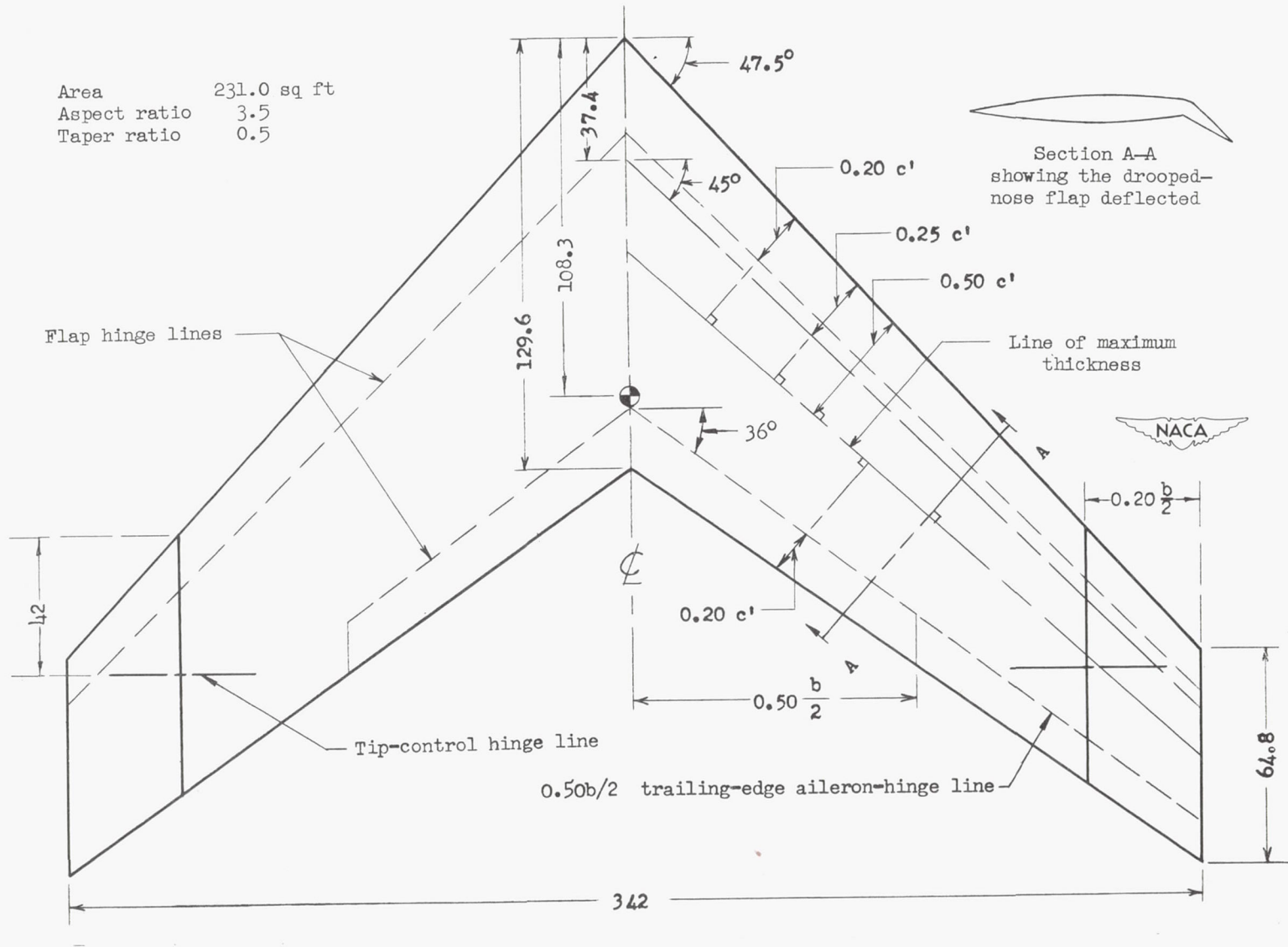


Figure 1.- Plan form of 47.5° sweptback wing. All dimensions are in inches.



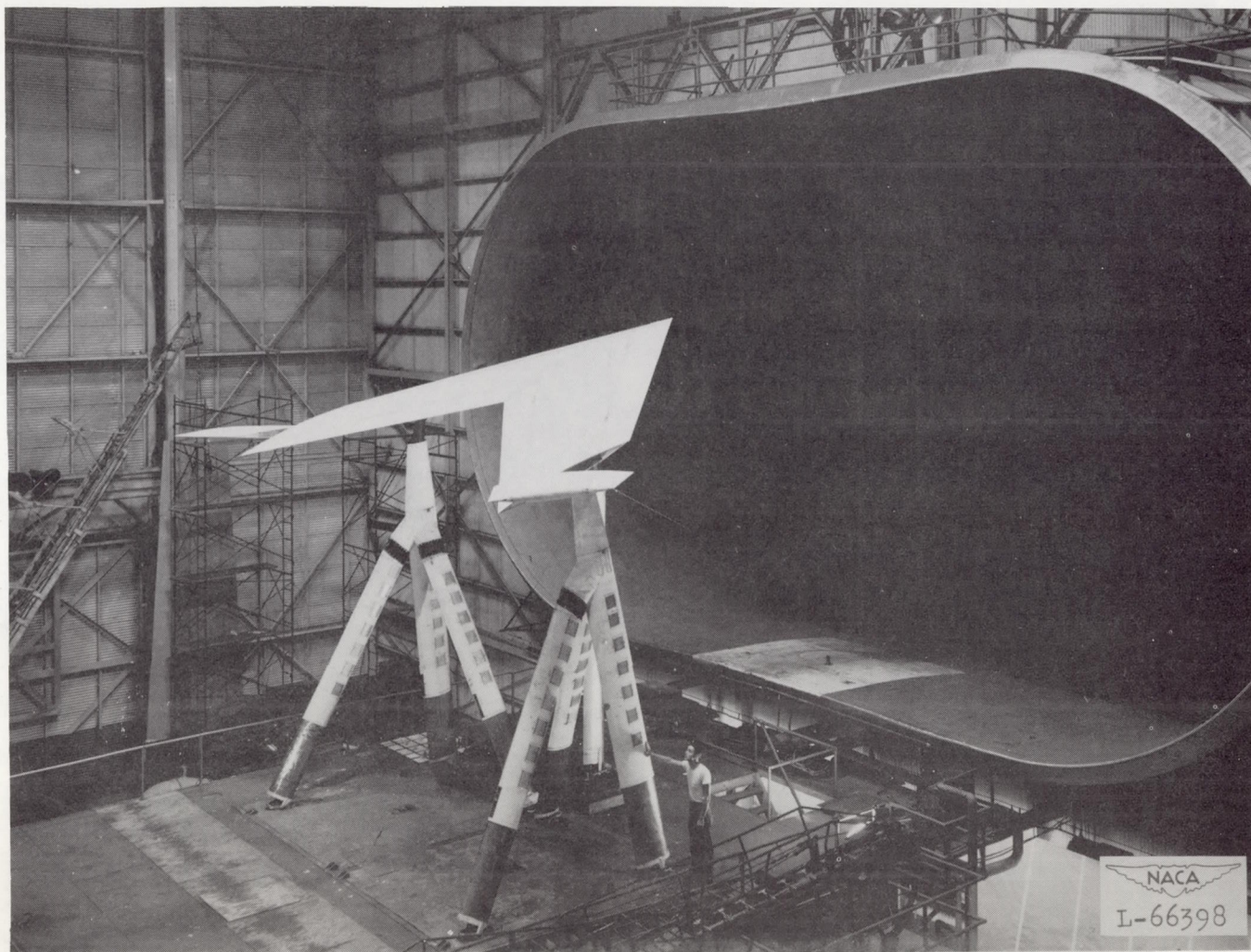
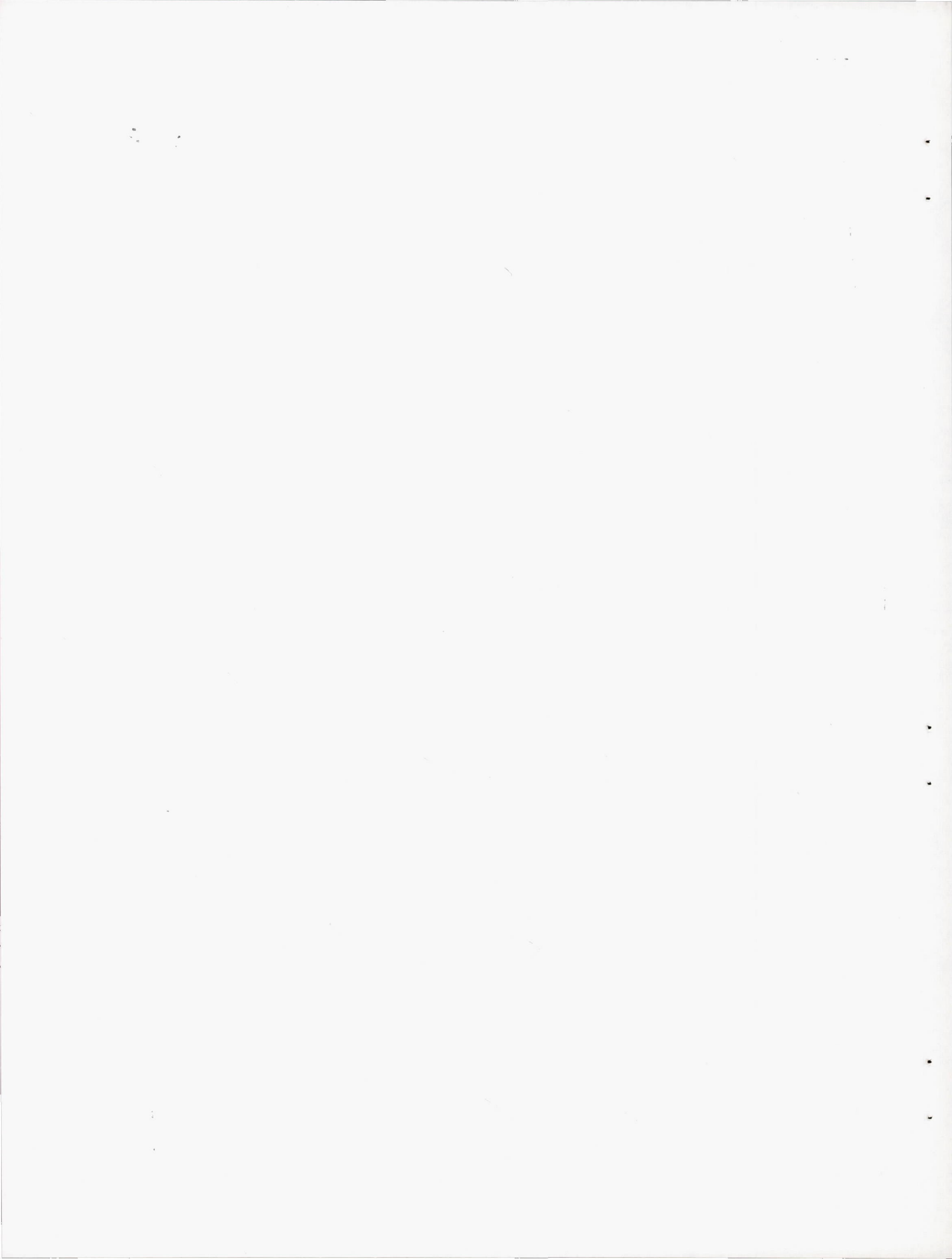
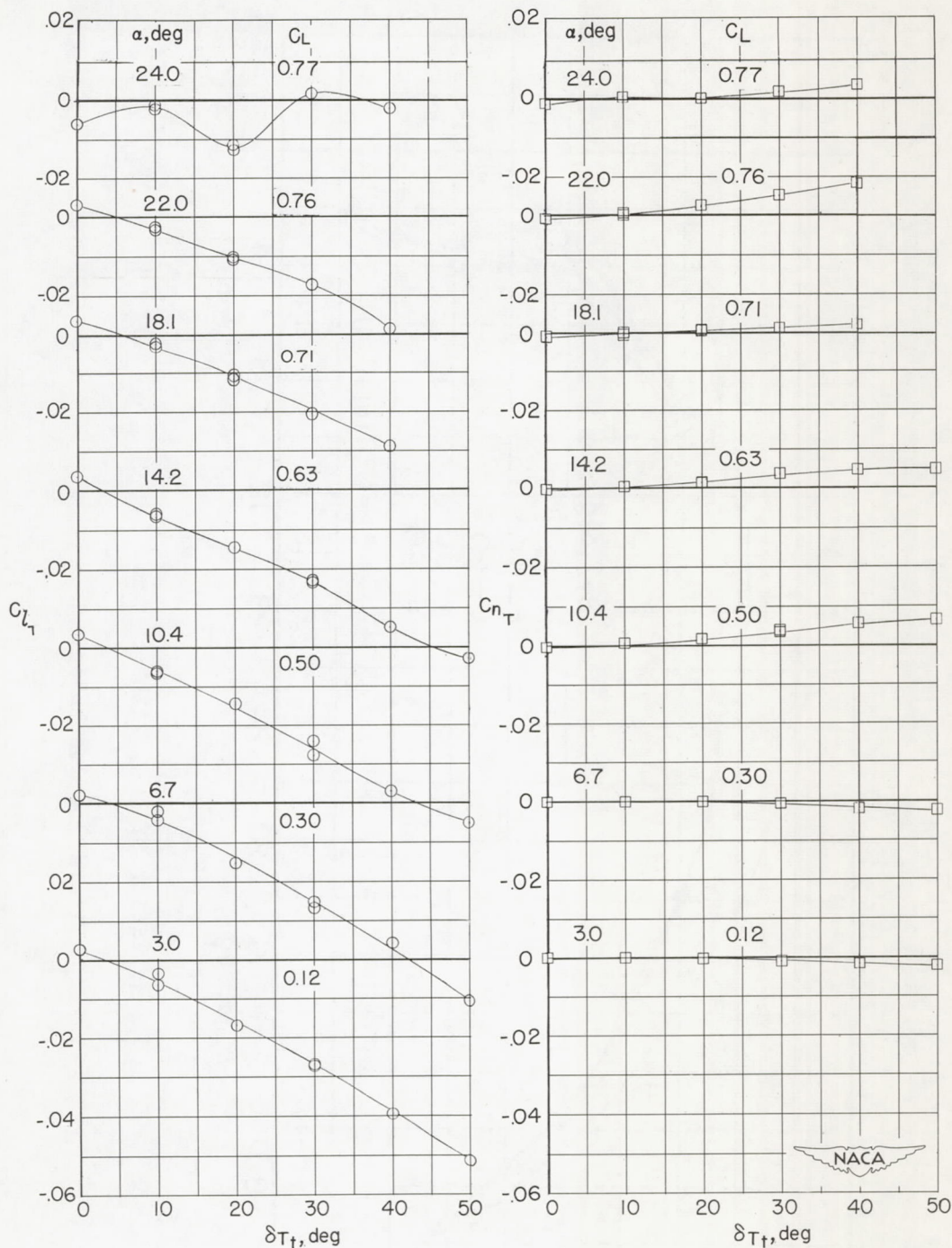


Figure 2.- Photograph of  $47.5^\circ$  sweptback wing mounted in the Langley full-scale tunnel with the tips deflected in the same direction.

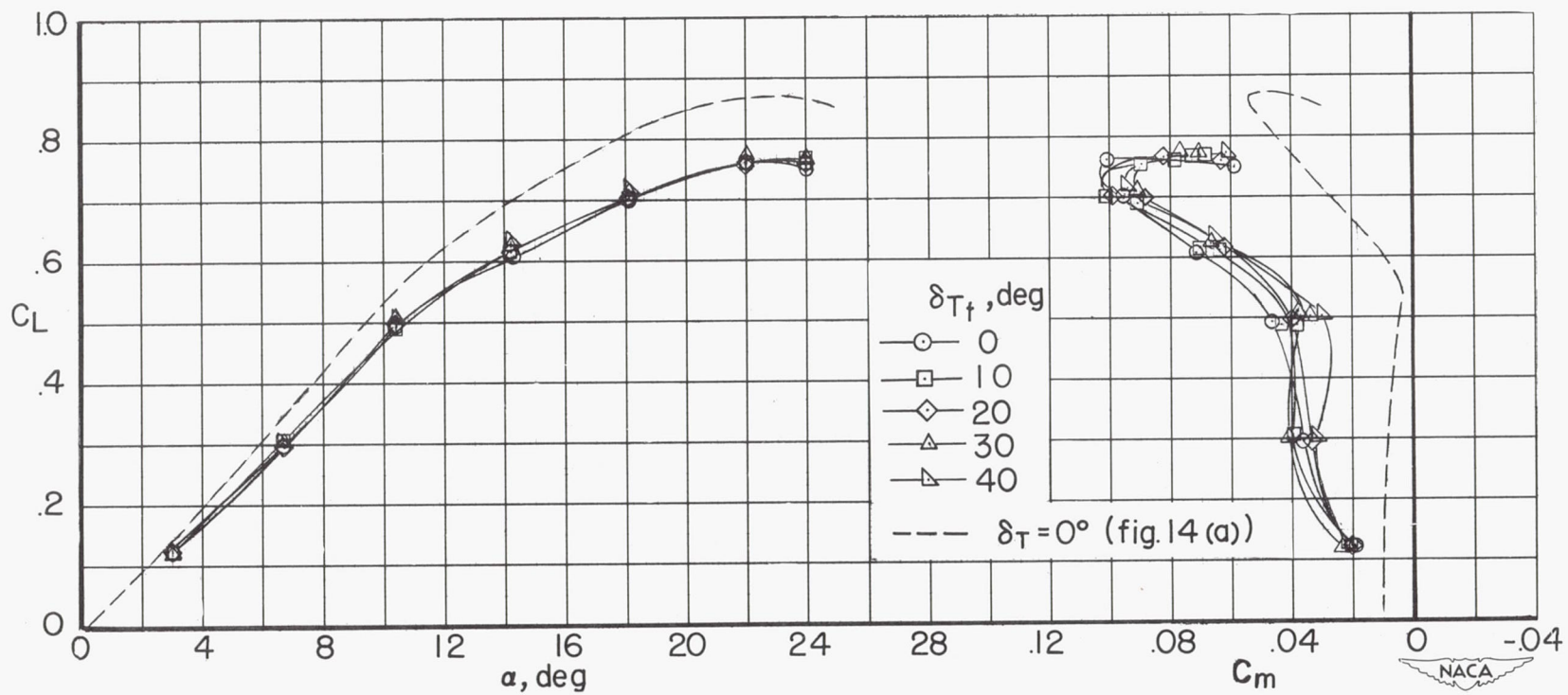






(a) Variation of  $C_{L_T}$  and  $C_{n_T}$  with  $\delta_{T_t}$ .

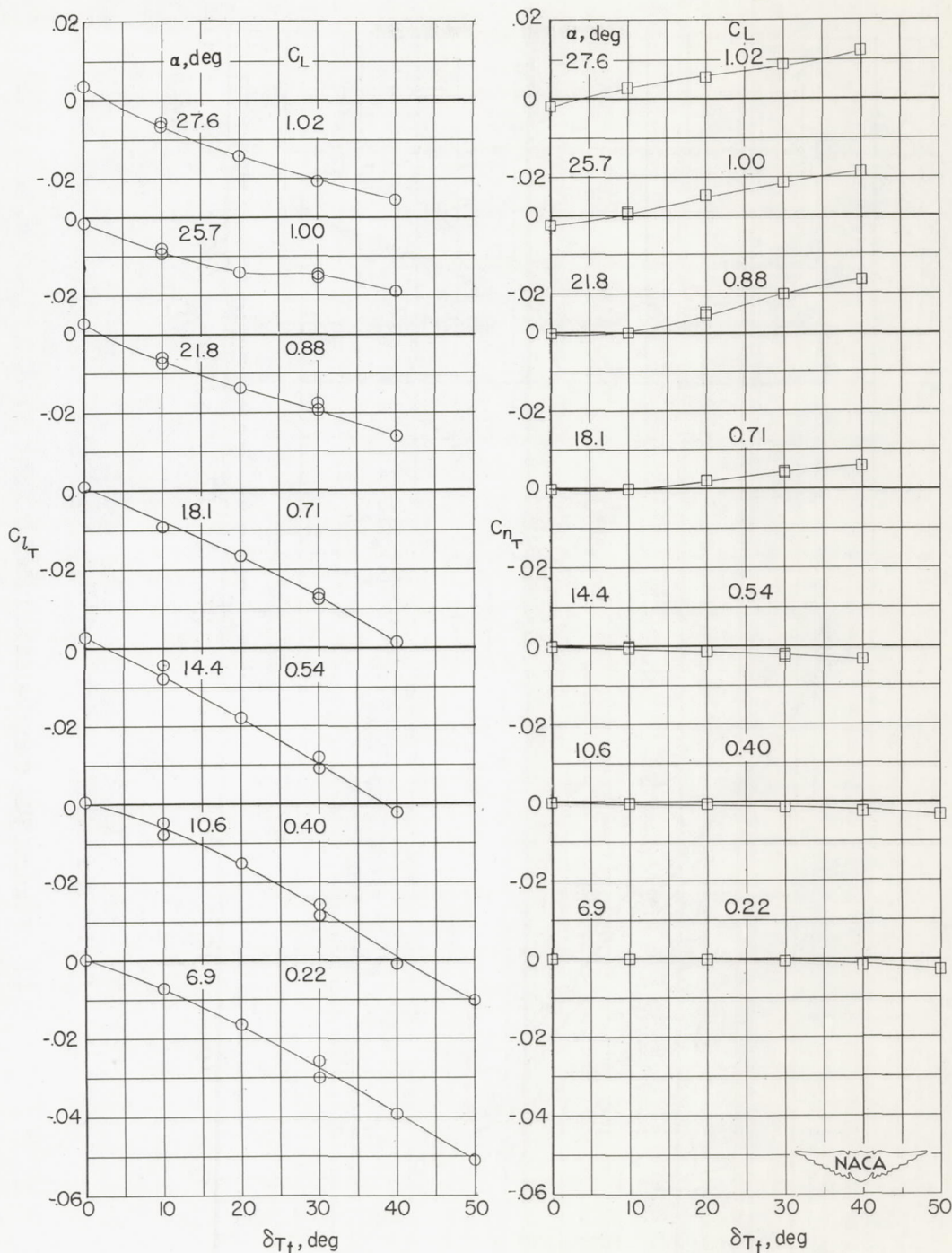
Figure 3.- Characteristics in left roll of the tip controls for the basic wing configuration.  $R \approx 4.3 \times 10^6$ . (See table I for initial tip deflection  $\delta_{T_t}$  for each angle of attack.)



(b) Variation of  $C_L$  with  $\alpha$  and  $C_m$ .

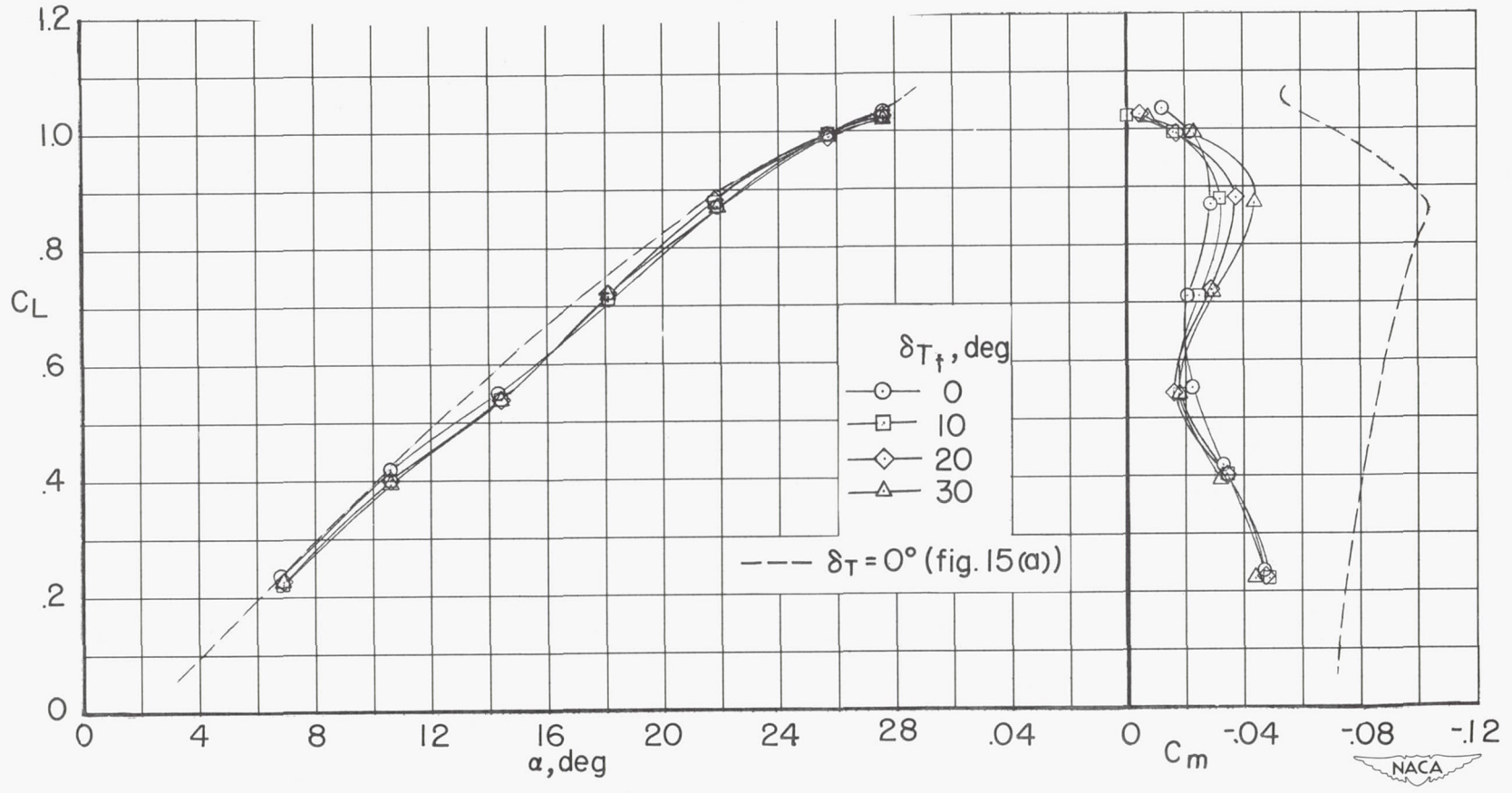
Figure 3.- Concluded.





(a) Variation of  $C_{l_T}$  and  $C_{n_T}$  with  $\delta_{T_t}$ .

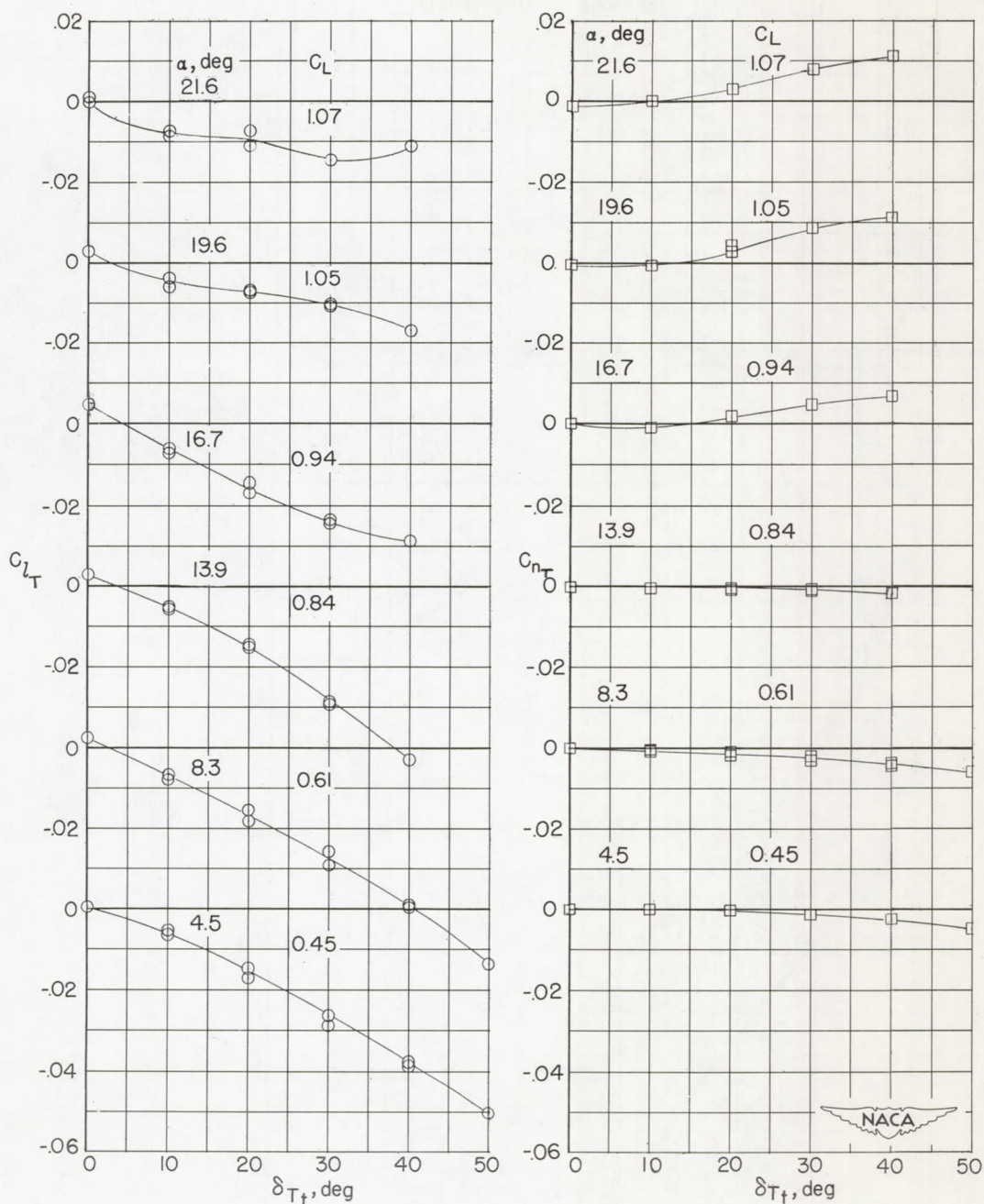
Figure 4.- Characteristics in left roll of the tip controls for the wing with  $0.80b/2$  drooped-nose flaps deflected  $40^\circ$ .  $R \approx 4.3 \times 10^6$ . (See table I for initial tip deflection  $\delta_{T_t}$  for each angle of attack.)



(b) Variation of  $C_L$  with  $\alpha$  and  $C_m$ .

Figure 4.- Concluded.

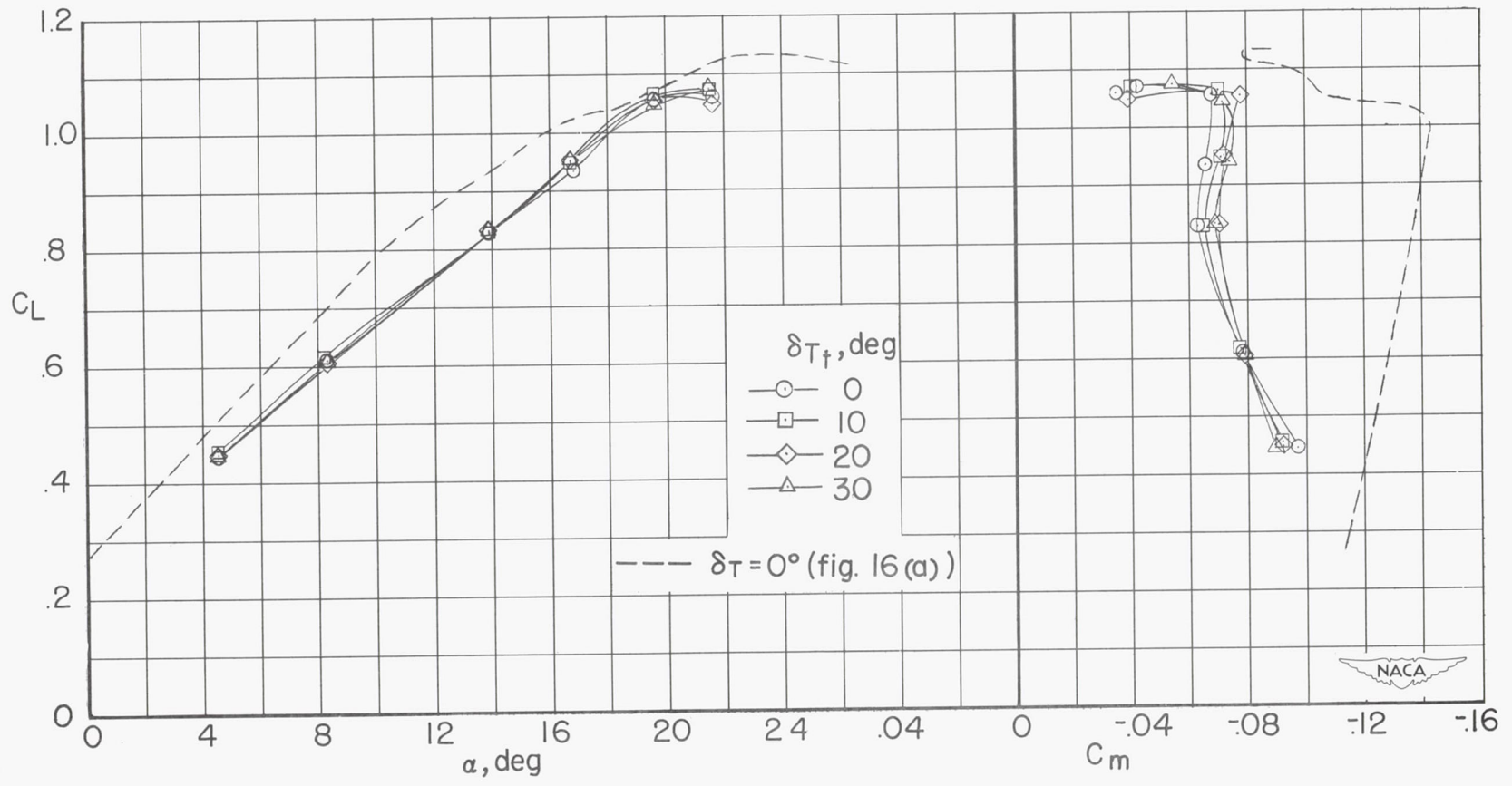




(a) Variation of  $C_{l_T}$  and  $C_{n_T}$  with  $\delta_{T_t}$ .

Figure 5.- Characteristics in left roll of the tip controls for the wing with  $0.80b/2$  drooped-nose flaps and semispan plain flaps deflected  $40^\circ$ .

$R \approx 4.3 \times 10^6$ . (See table I for initial tip deflection  $\delta_T$  for each angle of attack.)



(b) Variation of  $C_L$  with  $\alpha$  and  $C_m$ .

Figure 5.- Concluded.



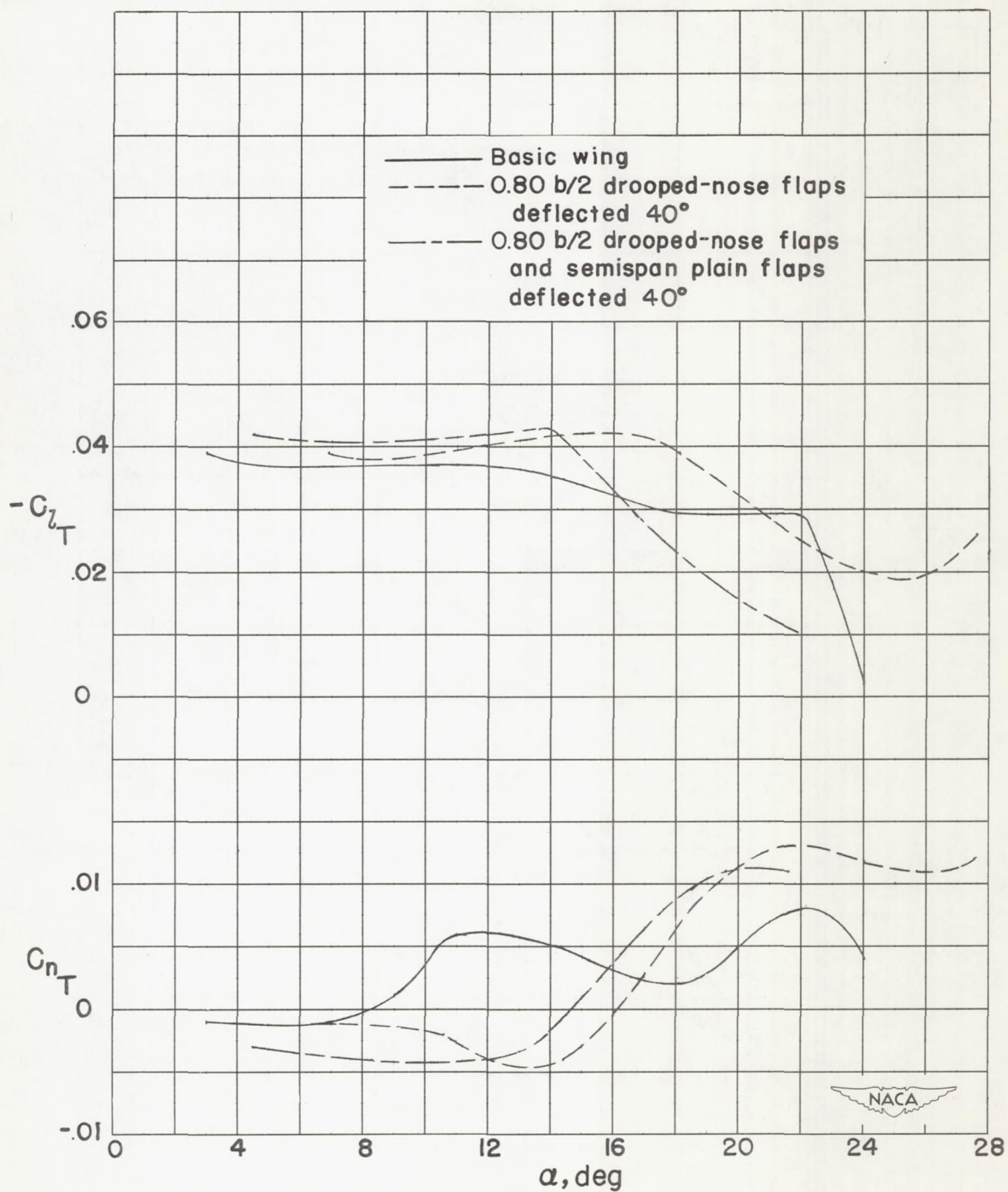


Figure 6.- Rolling- and yawing-moment characteristics for a total tip-control deflection of 40° in negative roll.

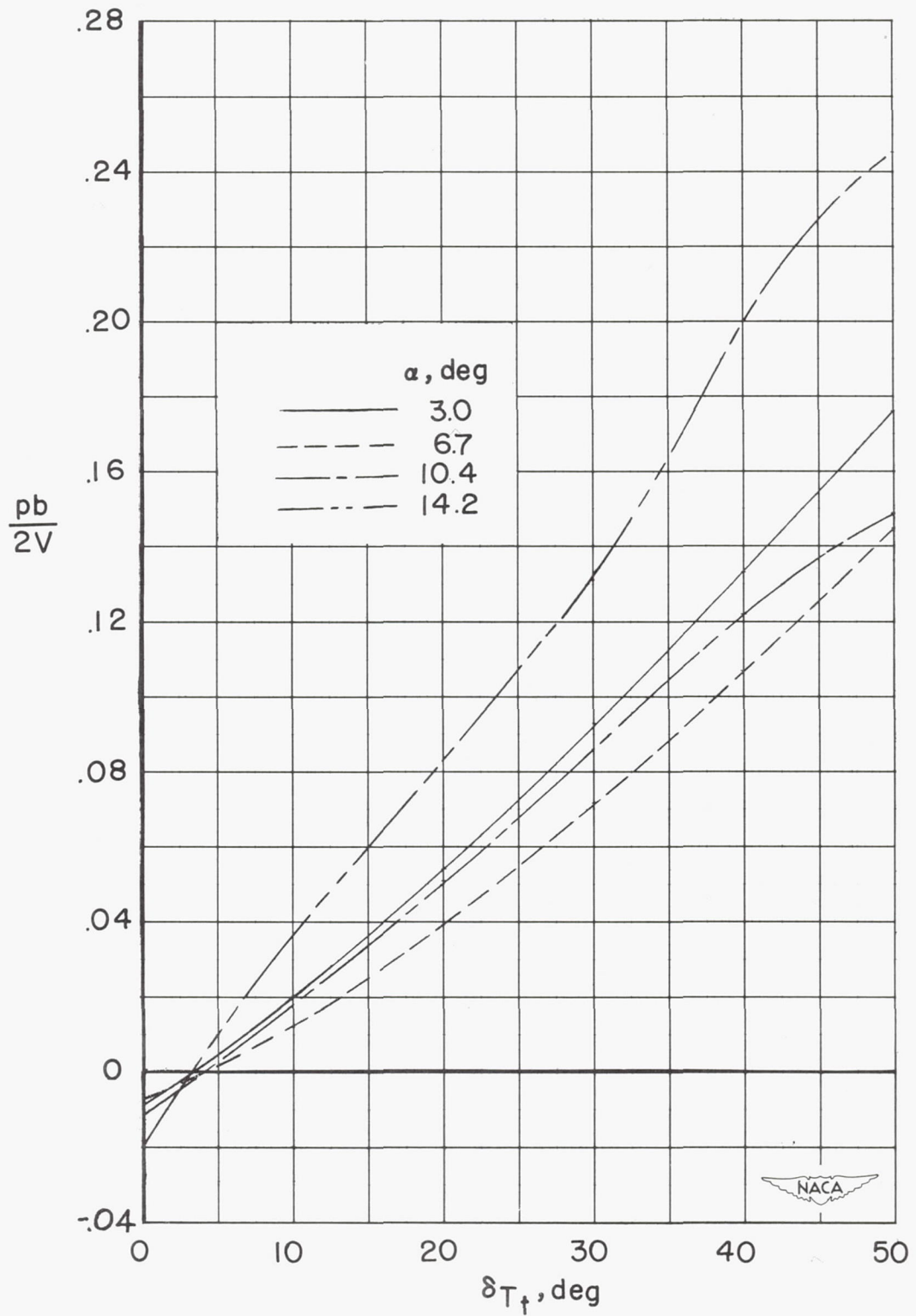


Figure 7.- Variation of estimated wing-tip helix angle  $\frac{pb}{2V}$  with total tip-control deflection for the basic wing.



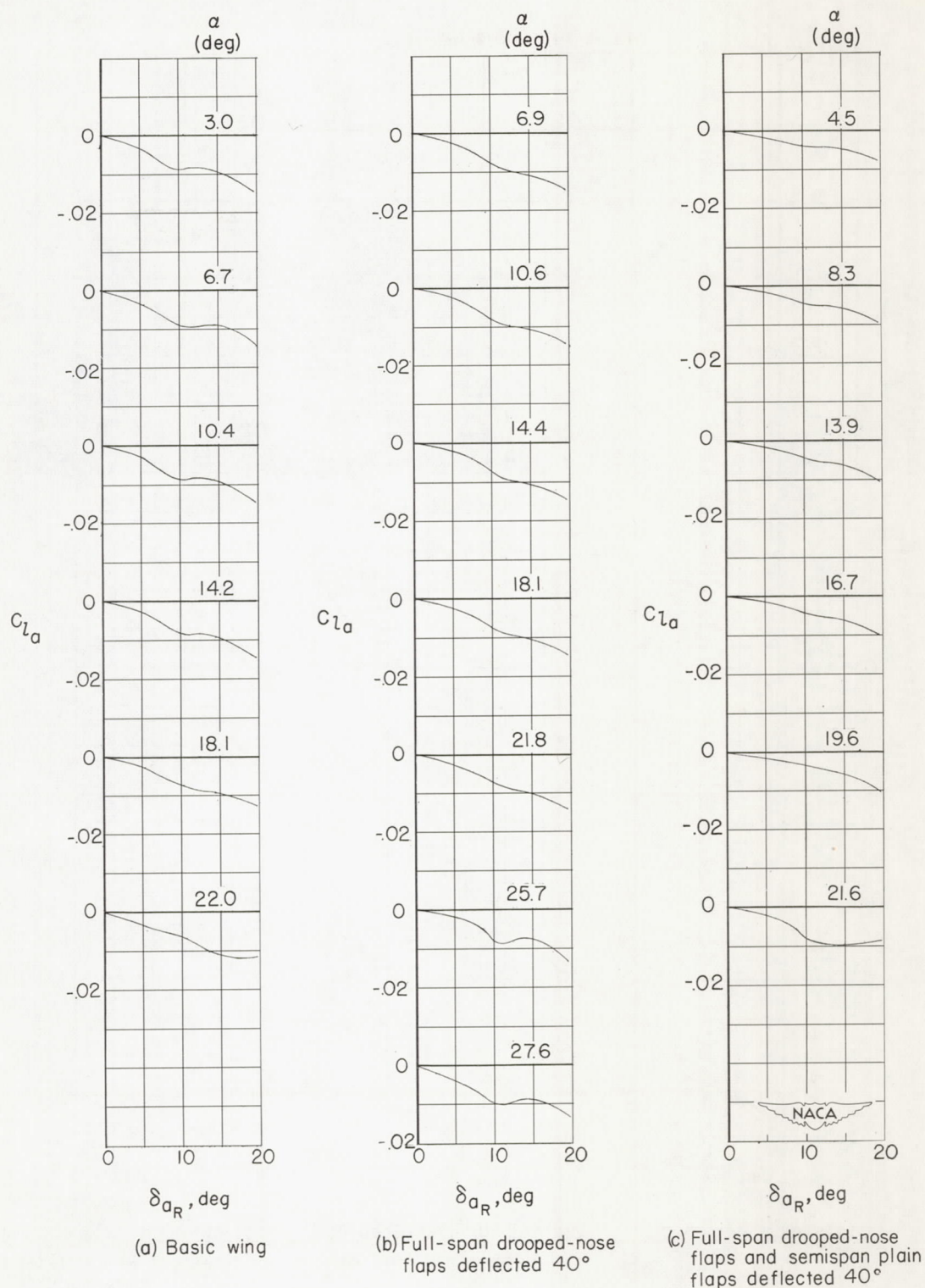
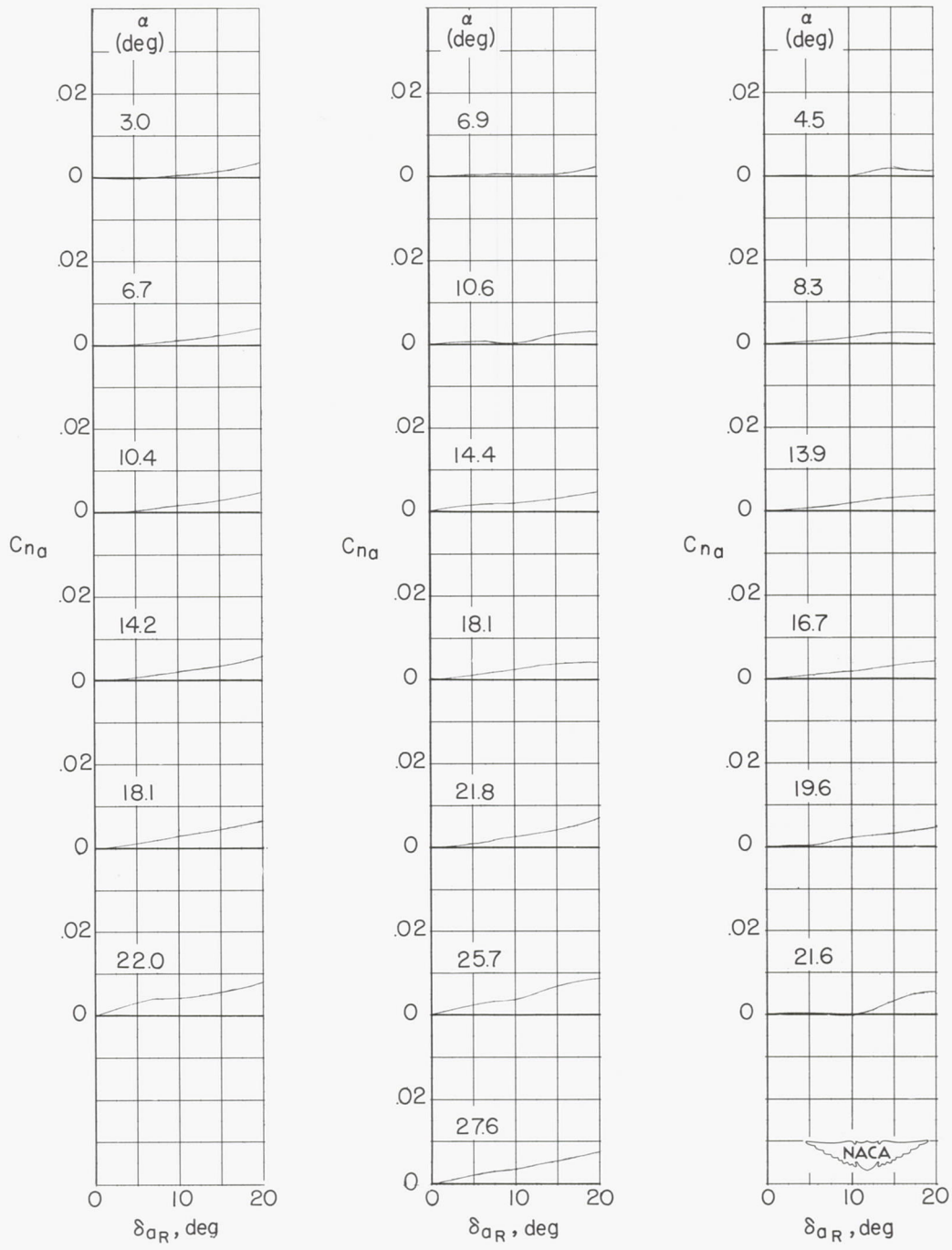


Figure 8.- Rolling-moment characteristics of the 0.50b/2 plain trailing-edge aileron.  $R \approx 4.3 \times 10^6$ .



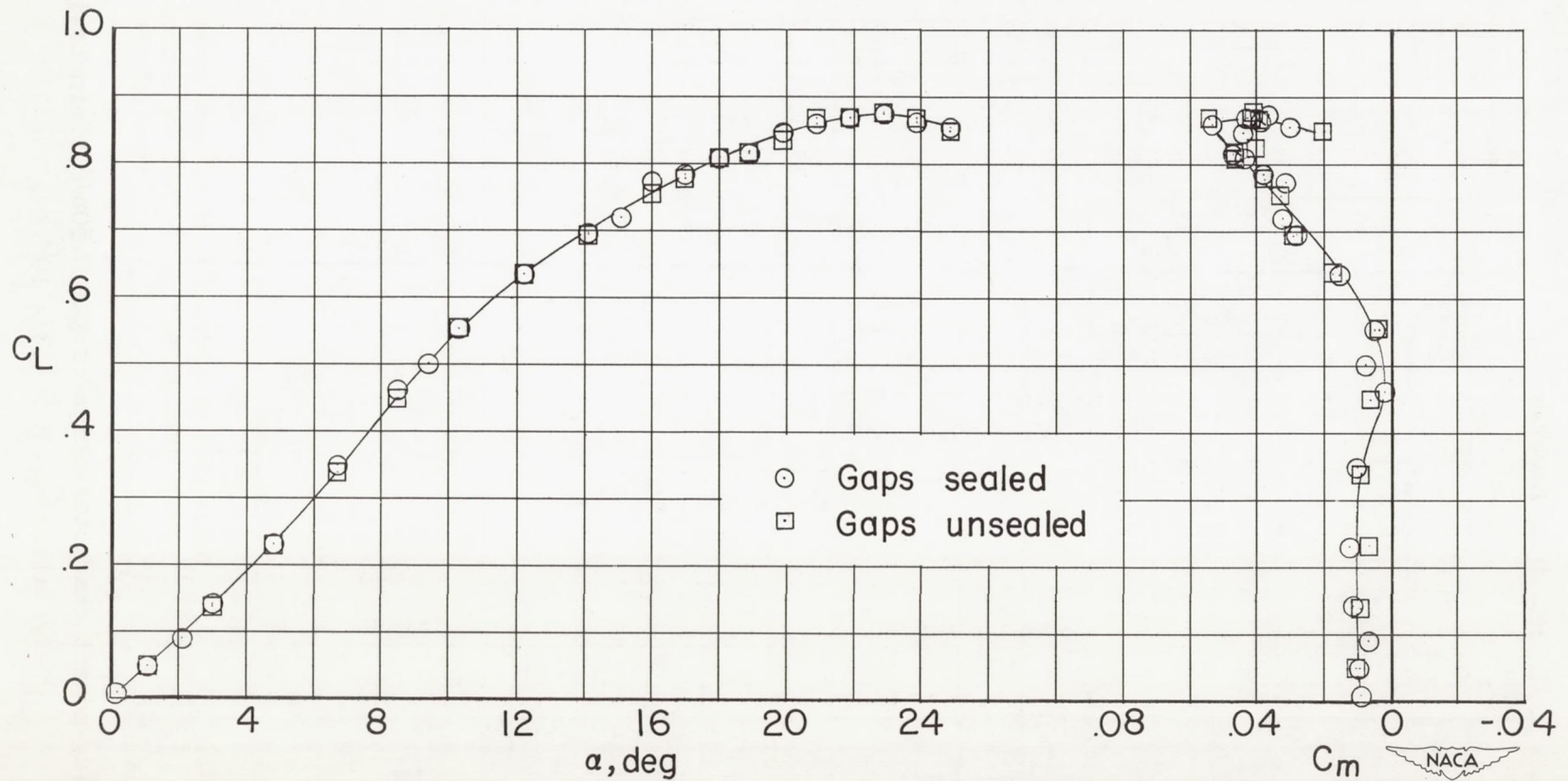
(a) Basic wing

(b) Full-span drooped-nose flaps deflected 40°.

(c) Full-span drooped-nose flaps and semispan plain flaps deflected 40°

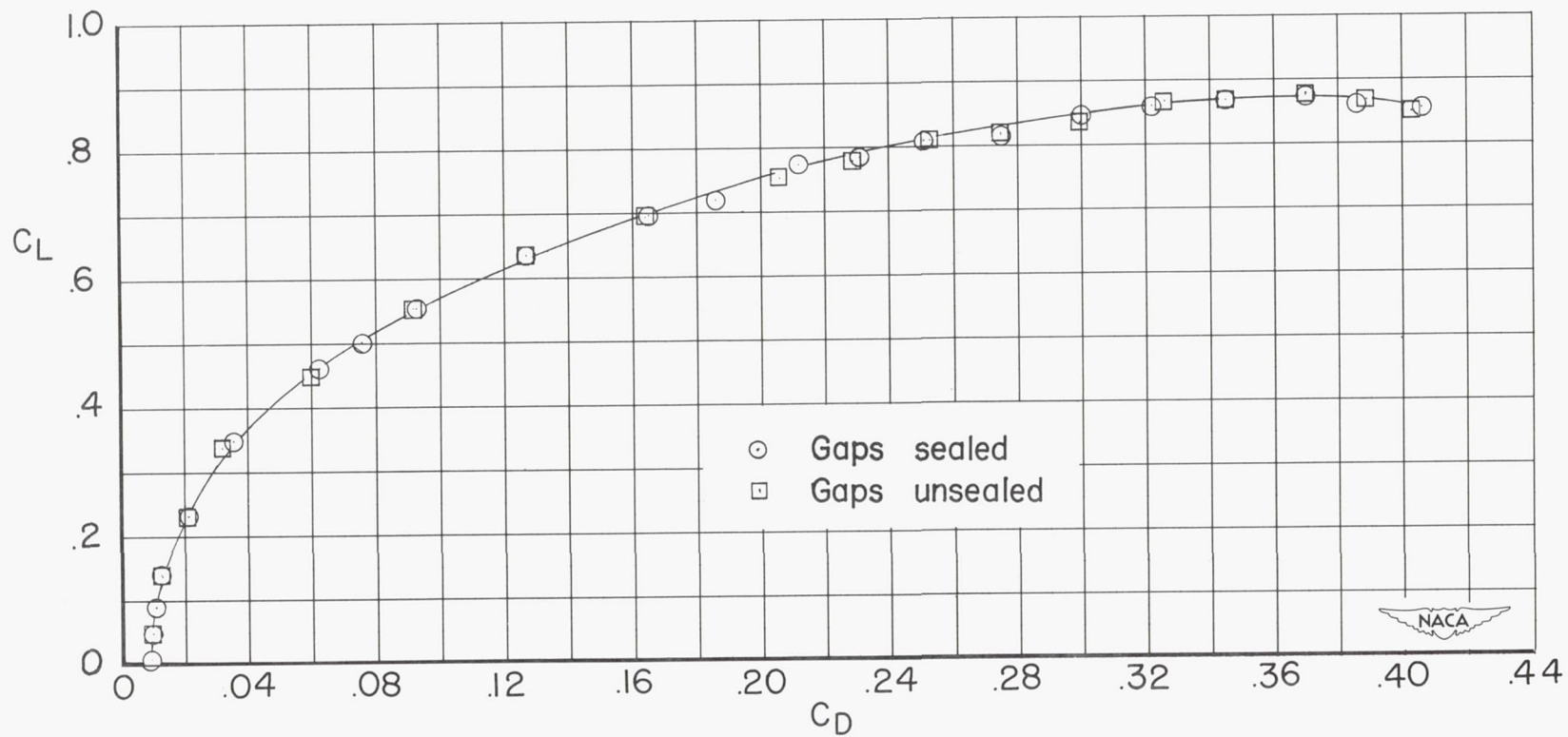
Figure 9.- Yawing-moment characteristics of the 0.50b/2 plain trailing-edge aileron.  $R \approx 4.3 \times 10^6$ .





(a) Variation of  $C_L$  with  $\alpha$  and  $C_m$ .

Figure 10.- Effect of the gaps at the junctures between tip controls and wing. Basic wing configuration;  $\delta_T = 0^\circ$ ;  $R \approx 4.3 \times 10^6$ .



(b) Variation of  $C_L$  with  $C_D$ .

Figure 10.- Concluded.

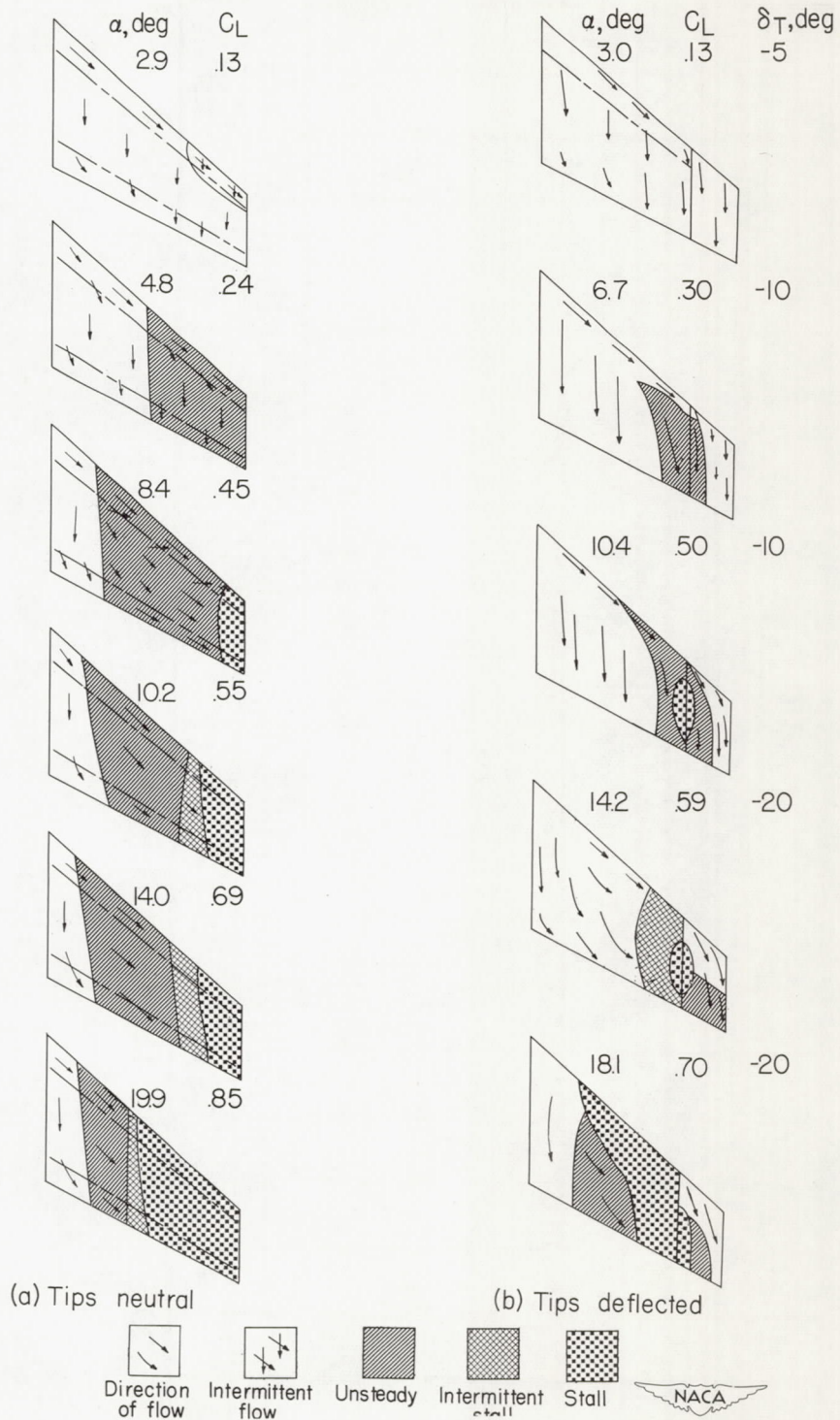


Figure 11.- Effect of tip deflection on the stalling characteristics of the basic wing configuration. Tip deflections for best flow improvement.  $R \approx 4.3 \times 10^6$ .



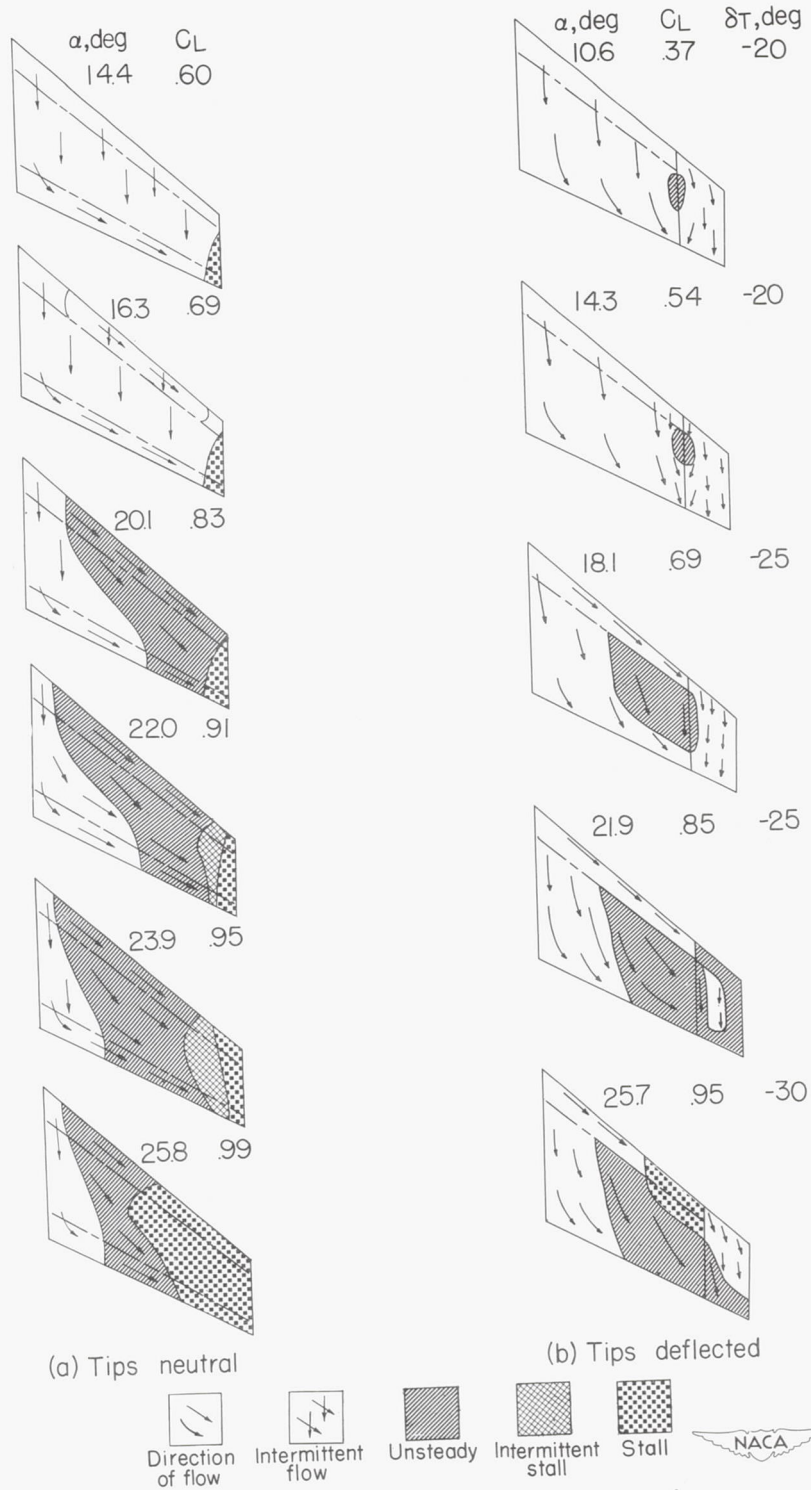


Figure 12.- Effect of tip deflection on the stalling characteristics of the wing with the drooped-nose flaps deflected  $40^\circ$ . Tip deflections for best flow improvement.  $R \approx 4.3 \times 10^6$ .

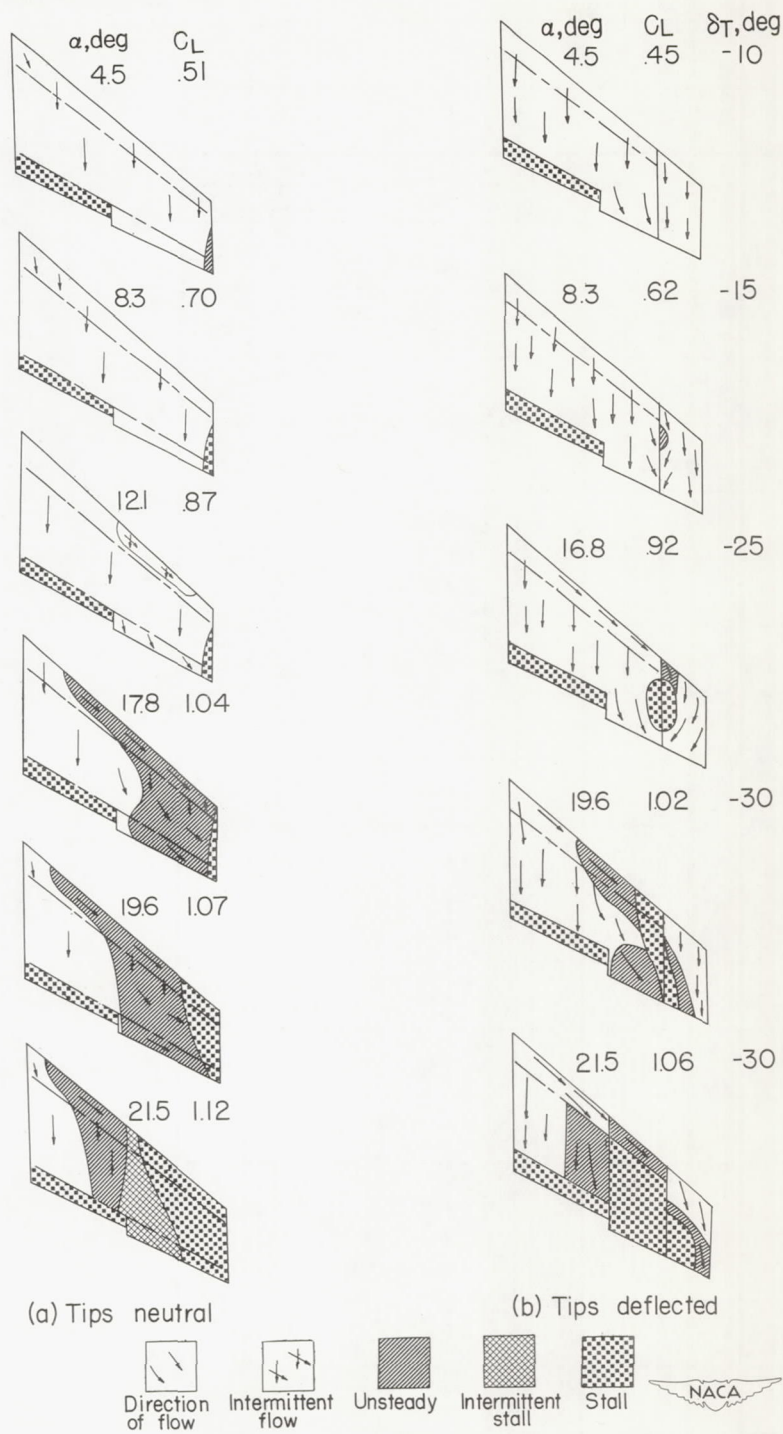
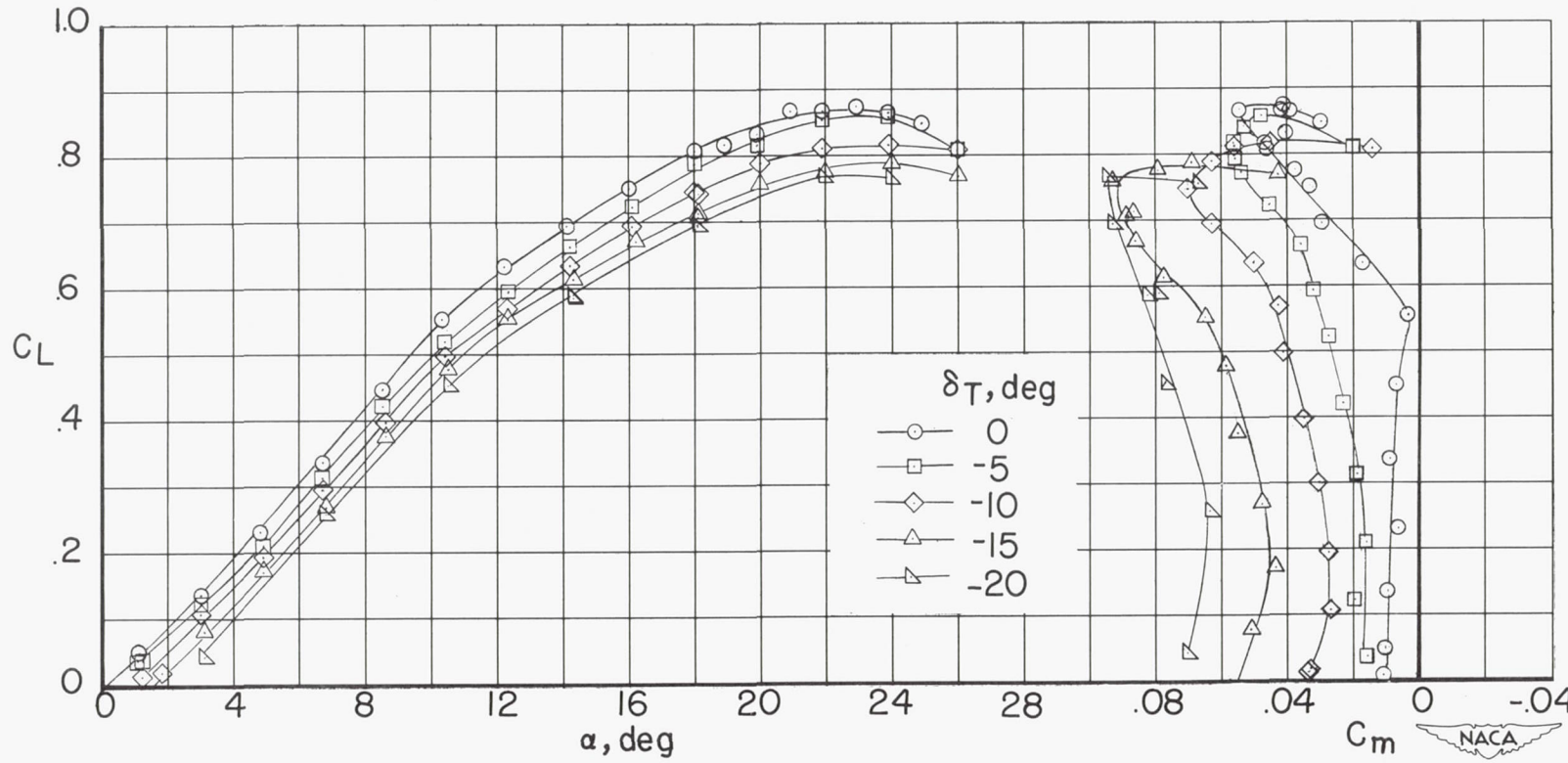


Figure 13.- Effect of tip deflection on the stalling characteristics of the wing with the drooped-nose flaps and semispan plain flaps deflected  $40^\circ$ . Tip deflections for best flow improvement.

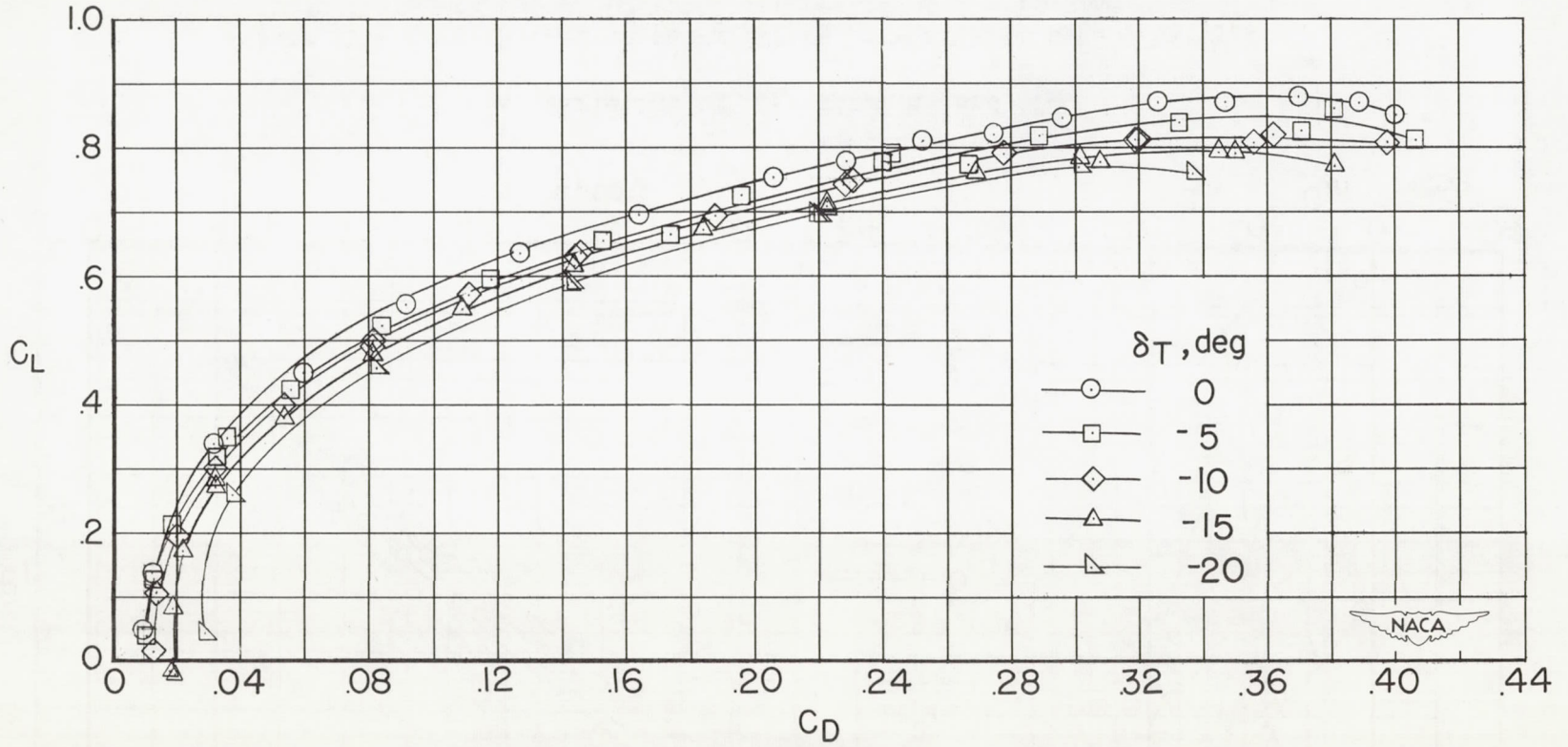
$R \approx 4.3 \times 10^6$ .



(a) Variation of  $C_L$  with  $\alpha$  and  $C_m$ .

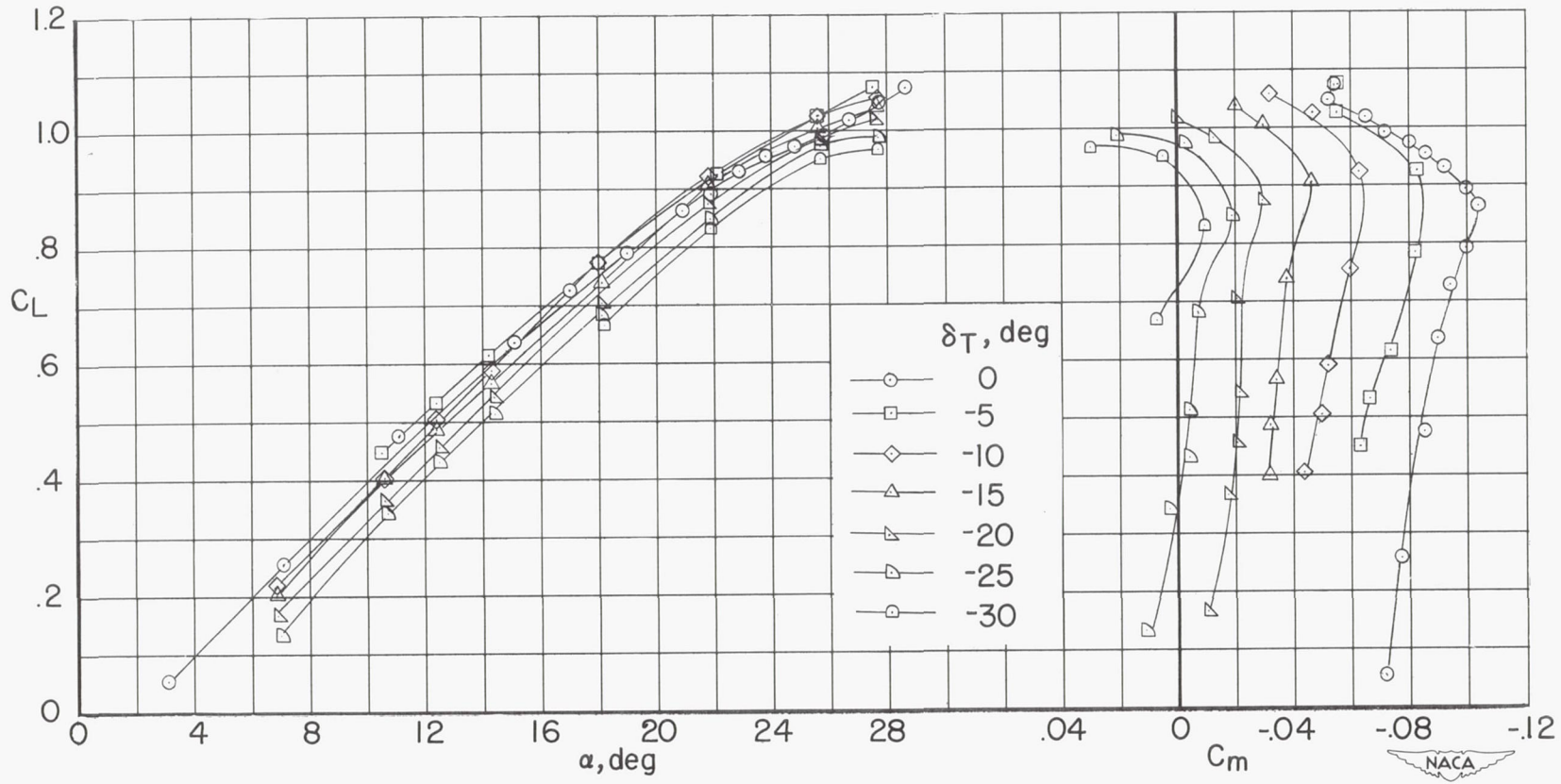
Figure 14.- Longitudinal characteristics of the basic wing with tips deflected in the same direction.  $R \approx 4.3 \times 10^6$ .





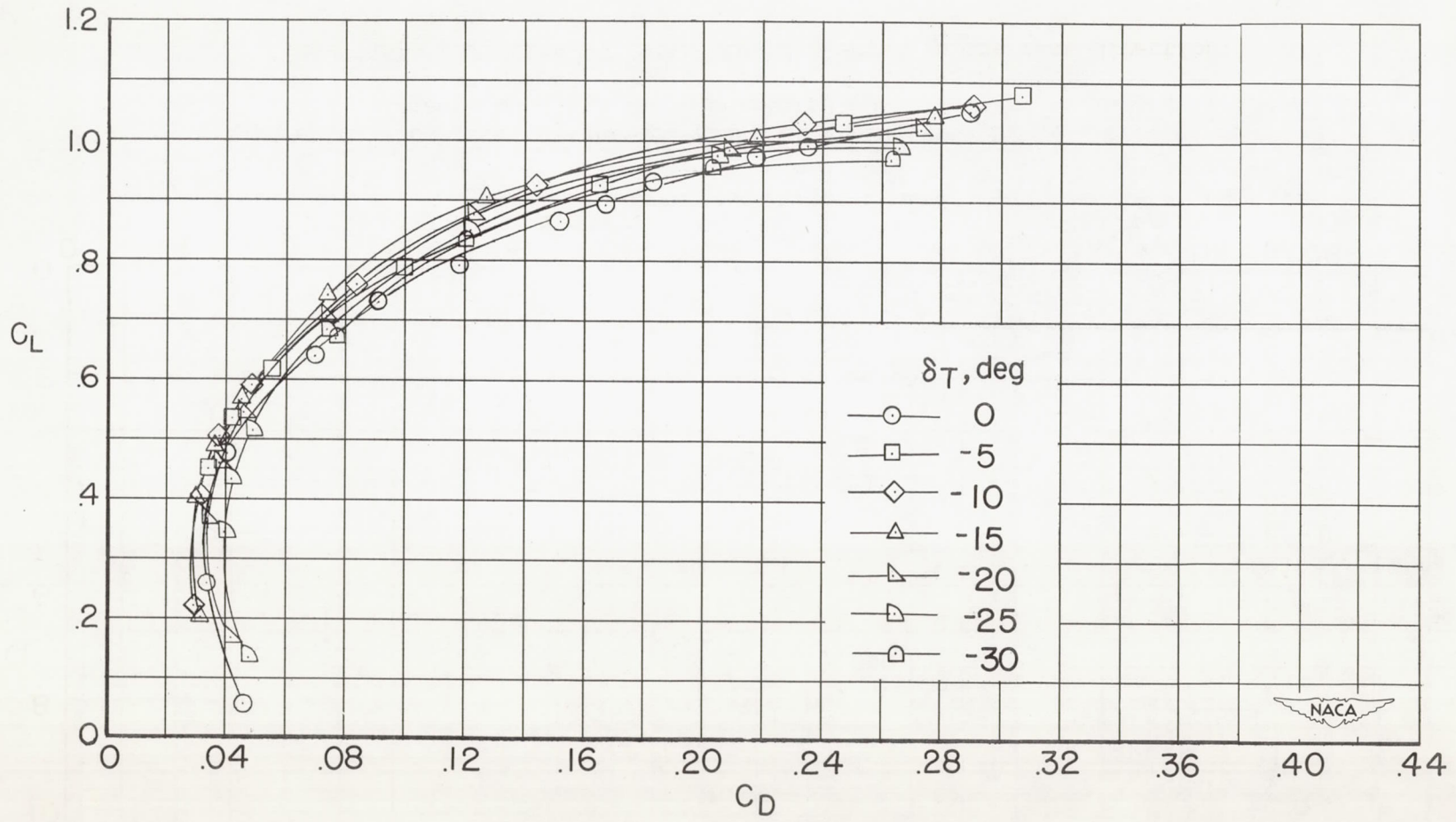
(b) Variation of  $C_L$  with  $C_D$ .

Figure 14.- Concluded.



(a) Variation of  $C_L$  with  $\alpha$  and  $C_m$ .

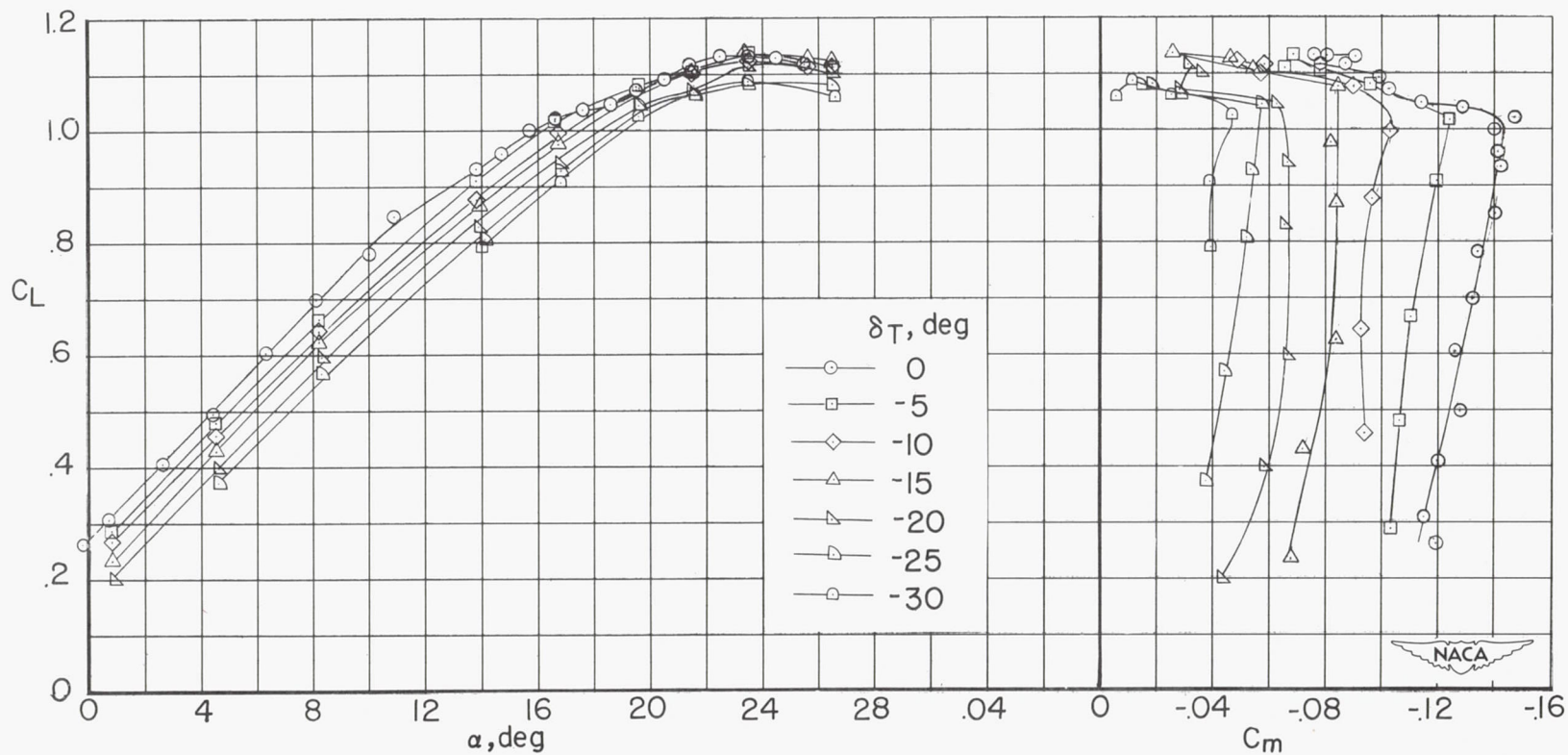
Figure 15.- Longitudinal characteristics of wing with  $0.80b/2$  drooped-nose flaps deflected  $40^\circ$  with tips deflected in the same direction.  
 $R \approx 4.3 \times 10^6$ .



(b) Variation of  $C_L$  with  $C_D$ .

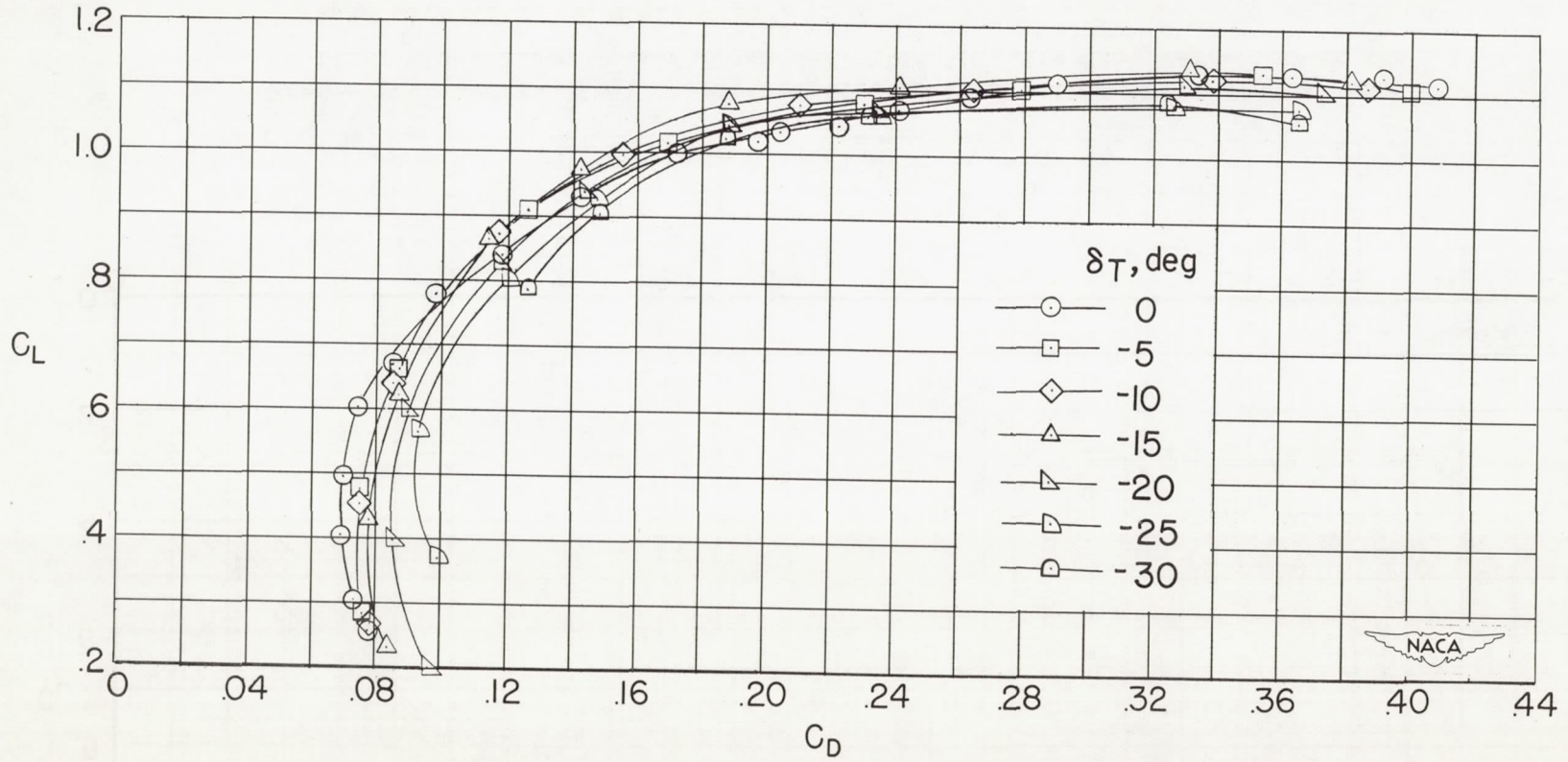
Figure 15.- Concluded.





(a) Variation of  $C_L$  with  $\alpha$  and  $C_m$ .

Figure 16.- Longitudinal characteristics of wing with  $0.80b/2$  drooped-nose flaps and semispan plain flaps deflected  $40^\circ$  with tips deflected in the same direction.  $R \approx 4.3 \times 10^6$ .



(b) Variation of  $C_L$  with  $C_D$ .

Figure 16.- Concluded.

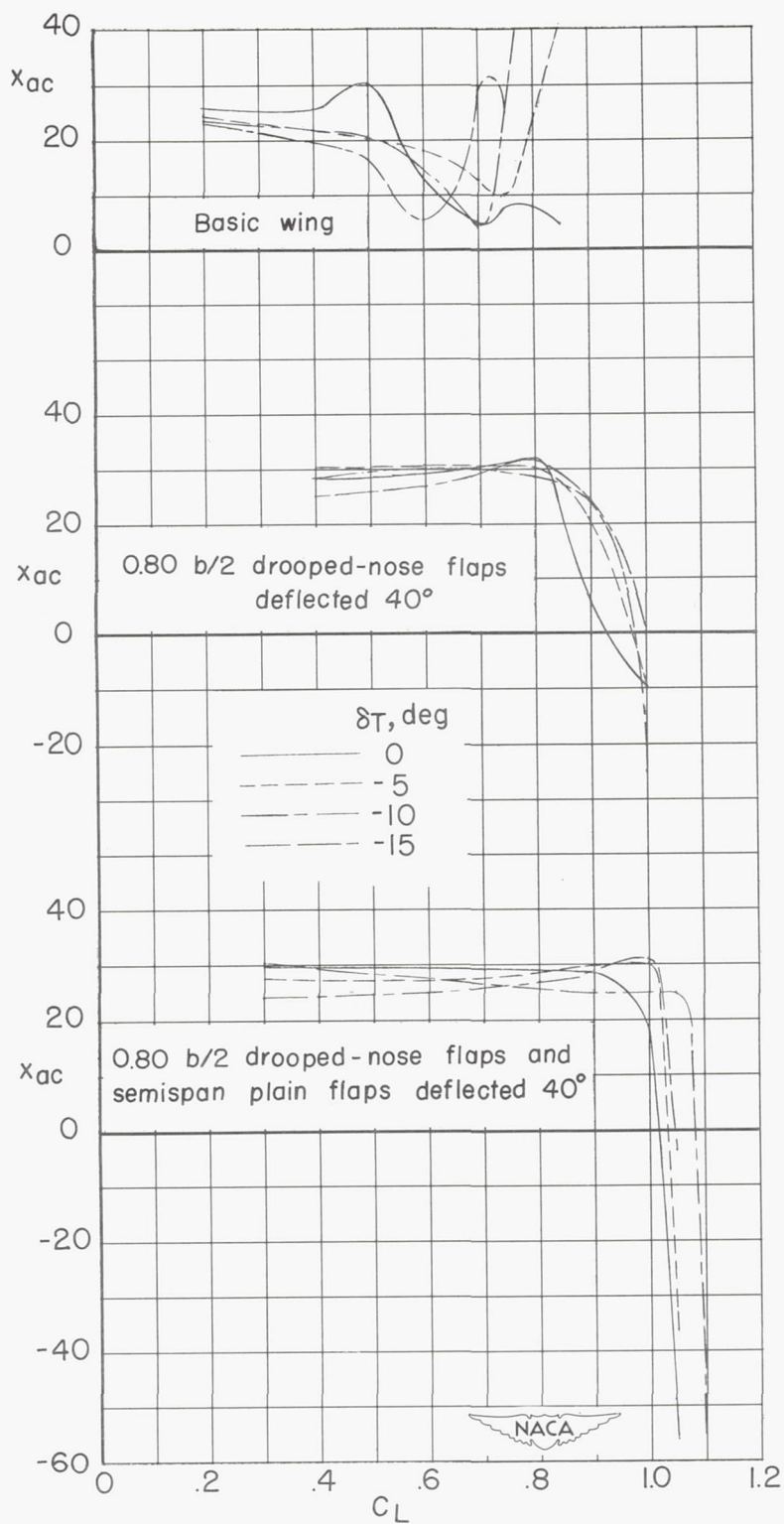
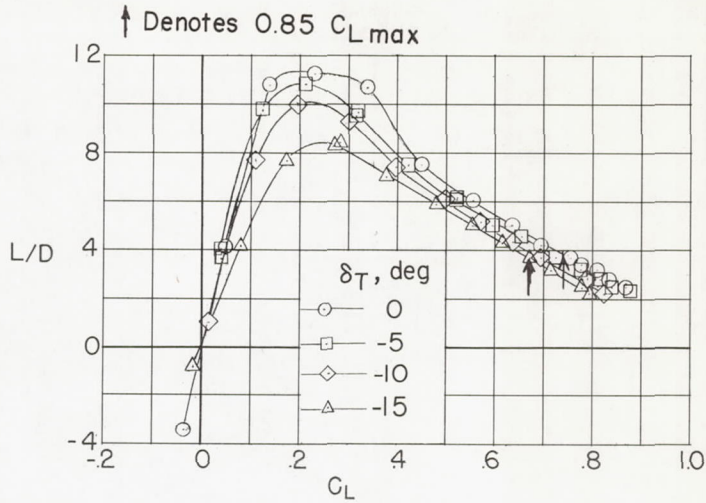
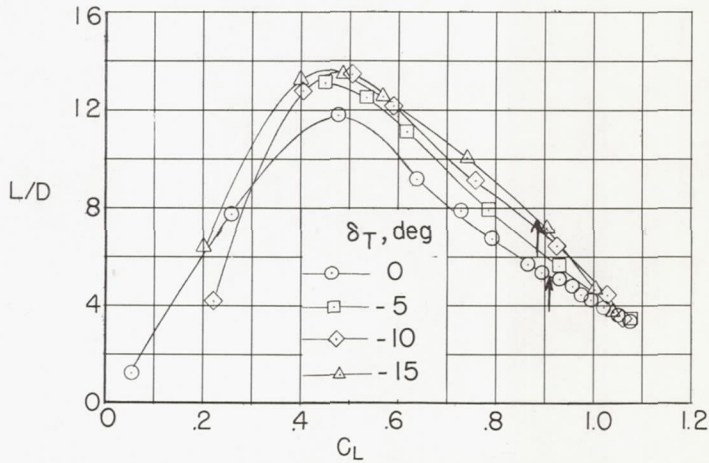


Figure 17.- Effect of tip-control deflection on the approximate aerodynamic-center location.  $R \approx 4.3 \times 10^6$ .

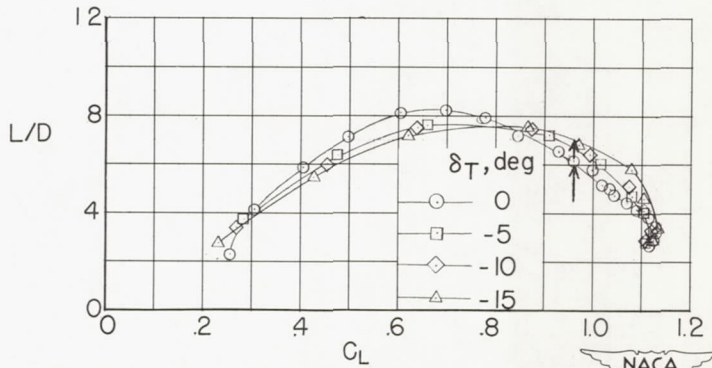




(a) Basic wing.



(b) 0.80  $b/2$  drooped-nose flaps deflected  $40^\circ$ .



(c) 0.80  $b/2$  drooped-nose flaps and semispan plain flaps deflected  $40^\circ$ .



Figure 18.- Effect of tip-control deflection on lift-drag ratio.

$$R \approx 4.3 \times 10^6.$$